doi:10.3304/JMES.2009.006

Journal of Mediterranean Earth Sciences **1** *(2009), 61-84*

J M E S

Journal of Mediterranean Earth Sciences

Stratigraphy, structural setting and burial history of the Messinian Laga basin in the context of Apennine foreland basin system

Sabina Bigi*, Salvatore Milli*, Sveva Corrado**, Piero Casero***, Luca Aldega**, Flavia Botti•, Massimiliano Moscatelli••, Olivier Stanzione°, Federico Falcini°°, Mattia Marini*, Domenico Cannata*

**Dipartimento Scienze della Terra, SAPIENZA Università di Roma, P.le A. Moro, 5 - 00185 Roma, Italy*
***Dipartimento di Scienze Geologiche, Università "Roma Tre", Largo San Leonardo Murialdo, 1 - 00146 Roma, Italy*
****Via di S. Martino Valperga, 20 - 00147 Roma, Italy*
•Dipartimento di Scienze della Terra, Università di Pisa, Lungarno Pacinotti, 43 - 56126 Pisa, Italy
••CNR-IGAG, Istituto di Geologia Ambientale e Geoingegneria, Via Salaria km 29,300 - 00016 Monterotondo Stazione, Roma, Italy
°Task Geoscience Ltd Enterprise House, Aberdeen, AB23 8GX, UK
°° Department of Earth and Environmental Science, University of Pennsylvania, 240 S. 33rd Street - Hayden Hall, Philadelphia, PA 19104-6316, USA

ABSTRACT - An integrated approach to the study of the Central Apennines thrust system has been conducted, combining together new field, geophysical, organic matter maturity and mineralogical datasets. The area comprises one of the most studied basins of the Central Apennines: the Laga basin. It developed during the Messinian time and represents the link between the internal, uplifted, Lower Miocene fold-and-thrust belt to the west, and the external, more recent part of the chain, buried below a thick pile of synorogenic, Plio-Pleistocene clastic deposits of the Periadriatic basin to the east. The Laga basin is filled by several turbiditic sedimentary sequences, largely studied in the past and mostly included into the Laga Formation, classically considered the fill of a deep marine foredeep basin connected to the flexure of the subducted Adriatic lithosphere under the Apennines. Our results clearly suggest that during Messinian, the main factor controlling depositional system architectures was thrusts activity, which governed the localization of the main depocenter in the basin and its eastward space-time migration. The occurrence of thrust activity during deposition of most of the Laga basin sedimentary succession suggests that it can be described as an internally deformed but not migrating sedimentary wedge, having features recording the transition from foredeep to wedge top depozone.

KEY WORDS: foredeep, wedge top basin, fold-and-thrust belt, basin analysis, sequence stratigraphy, Central Apennines

Submitted: 16 october 2009 - Accepted: 20 november 2009

INTRODUCTION

Foreland basins form on the continental crust at the front of active thrust systems, and, as a consequence, constitute sectors characterised by high tectonic mobility. In the foreland, basin sedimentation is controlled by two opposite mechanisms: uplift, due to forward propagation of the orogenic wedge, and flexural subsidence, under the orogenic wedge and/or subsurface loading (Beaumont, 1981; Karner and Watts, 1983; Ori and Friend, 1984; Royden and Karner, 1984; Allen and Homewood, 1986; Ricci Lucchi, 1986; Fleming and Jordan, 1990; De Celles and Giles, 1996; Ford, 2004). Most of the accommodation space is the result of flexural subsidence and is strictly correlated to the curvature of the subducted plate and to the position of the orogenic wedge with respect to the hinge of subduction (Doglioni et al., 2006 and references therein). This tectonic model provides the coexistence of different depozones that from the orogenic wedge to the foreland are (Fig. 1): 1) a wedge top depozone where sedimentation is strongly controlled by thrust activity, 2) a foredeep depozone, further subdivided into inner, axial and outer foredeep (Artoni et al., 2000; Mutti et al., 2003), characterized by shallow and/or deep marine sedimentation depending on the evolution of the foreland system, and 3) an outer ramp marking the passage from foredeep to foreland depozone, where most of the foredeep turbidite system onlapped (Fig. 1). The vertical passage between these sectors occurs through the progressive deformation and migration of the entire foreland basin system, and is marked by a vertical change of depositional systems: deep-water turbidite systems should characterise the lower portion of the sedimentary succession (foredeep depozone), passing upward to mixed turbidite and deltaic depositional systems (wedge top depozone), and finally to continental deposits, testifying an overall progradational trend toward the foreland (see Mutti et al., 2003 and references therein). It is clear that depending on the sector of the foreland basin, the vertical change from foredeep to wedge top sedimentation is often difficult to be recognised in the field, and it is evident that such a change occurs within a time lapse varying from basin to basin. Reasonably, the change from foredeep to wedge top depozone inevitably implies a size reduction of the foredeep basin and its internal structuring through the growing of the internal and more external thrusts, leading to a modification of the basin morphology, that in turn influences the direction of the turbidite flows and the resulting facies.

*Corresponding author: *sabina.bigi@uniroma1.it*

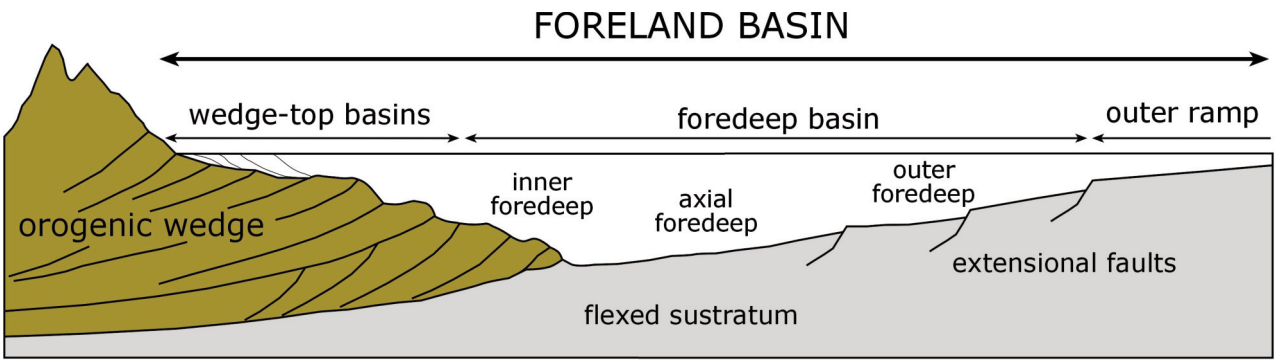

Fig. 1 - Schematic cross-section of a foreland basin system. Modified after De Celles and Giles (1996); Artoni et al. (2000); Mutti et al. (2003).

In the Central Apennines, features such as growing anticlines, intra-basin ridges and syn-sedimentary normal faulting have been recognised by several Authors, and related to a complex foreland geometry (see e.g. Corrado, 1995; Milli and Moscatelli, 2000; Mazzoli et al., 2002; Tozer et al., 2002; Artoni, 2003, 2007; Bigi et al., 2003; Bigi and Costa Pisani, 2005; Milli et al., 2007). In this paper such features, just recognised in the upper Tortonian-Messinian Laga Basin are described with more detail using an integrated methodological approach comprising: i) physical stratigraphic and sedimentological data, ii) interpretation of the available seismic dataset, and iii) thermal maturity data derived from organic matter and clay mineralogy analyses and are utilized to better understand how the passage from foredeep depozone to wedge top depozone occurs.

GEOLOGICAL FRAMEWORK

The Apennine is a Late Oligocene to Present fold-and-thrust belt (Fig. 2), where the west-directed subduction of the continental Adriatic plate (a plate originating from the former meso-cenozoic passive continental margin of Africa plate) underneath the European plate, is responsible for the progressive eastward migration of thrusting and late extensional faulting which overprints and/or inverts former thrusts (Ricci Lucchi, 1986; Argnani and Ricci Lucchi, 2001; Carminati et al., 2004).

In the Northern Apennines, the stratigraphic succession is fundamentally made up of shallow-water and basinal carbonates and siliciclastic deposits (Umbria-Marche succession). Thrusts have an arched trend and are progressively younger eastward. Correlation among the ages of the active thrust front, the onset of the foredeep basin and the wedge top basin deposition has been reconstructed by several Authors (Patacca and Scandone, 1989; Boccaletti et al., 1990; Artoni and Casero, 1997; Bigi et al., 1995, 1999; Cipollari and Cosentino, 1995; Argnani and Ricci Lucchi, 2001; Casero, 2004). The amount of shortening calculated for the Northern Apennines is approximately 30-40%, while the average deformation rate is approximately 10 cm/yr; the less conservative geological sections reach values of 20 cm/yr (Bally et al., 1986; Mostardini and Merlini, 1986; Calamita et al., 1991; Ghisetti et al., 1993).

The structural style of the Central Apennines consists of faulted and tilted monoclines of shallow-water carbonate platform successions (Latium-Abruzzi carbonate platform). The main thrusts have a general NW-SE trend, and in some cases show geometric and kinematics relationships related to "out of sequence" thrusts. In this domain, chronology of turbidite foredeep deposits is not regularly related to the active thrust fronts and depocenters migration (Corrado et al., 1995; Ghisetti and Vezzani, 1997; Bigi and Costa Pisani, 2005 and references therein). The compressive deformation in the carbonate platform domain of the Central Apennines developed in a shorter time span (Tortonian-Upper Pliocene) than that which occurred in the Northern Apennines (pelagic domain; Oligocene-Recent?).

In the Laga basin above the mentioned carbonate substratum, a Tortonian-Messinian succession, made up of siliciclastic turbidites crops out (Fig. 3). The part of the Laga basin that was investigated, is located to the north of the Gran Sasso thrust and to the east of the Mt. Sibillini thrust; it is split up in an eastern and a western sector by the Montagna dei Fiori-Montagnone anticline. Moreover, two other main structures are recognizable: the Acquasanta anticline and the Gorzano normal fault (Centamore et al., 1991). The whole Laga basin domain tectonically overlies onto the Lower Pliocene deposits along the T1 thrust (Fig. 3).

The turbidite succession of the Laga basin deposited since late Tortonian when the ensuing propagation of the Apennine compressive thrust front led to the progressive fragmentation and reorganization of the Marnoso-arenacea foreland basin system. The final involvement in the thrust belt occurred during the intra-Messinian regional tectonic phase, which should mark, in our interpretation, the passage to the subsequent Upper Messinian to Present foreland basin system (Roveri et al., 2002, 2003; Manzi et al., 2005; Milli et al., 2007). The Laga turbiditic succession recorded this transitional phase, the Lower Messinian portion being representative of the closure phase of the Marnoso-arenacea foreland basin system and the upper Messinian portion representative instead of the onset of the present day foreland basin system.

PHYSICAL STRATIGRAPHY

The location of the Laga Basin in the context of the Apennine chain is crucial as it lies between important key tectonic elements (see previous paragraph). Consequently, understanding the stratigraphic-depositional stacking pattern of this basin provides important constraints a) on the local tectonic and climatic control on turbidite sedimentation, and b) on the tectonic evolution of the chain.

Messinian turbidite succession filling the Laga basin lies on Tortonian-Lower Messinian pelagic and hemipelagic deposits (Marne a Pteropodi and Marne a Orbulina Formations), and was originally interpreted as a classical deep-sea fan succession (Mutti et al., 1978). It was subdivided into three members, pre-evaporitic, evaporitic and post-evaporitic, and was further subdivided into

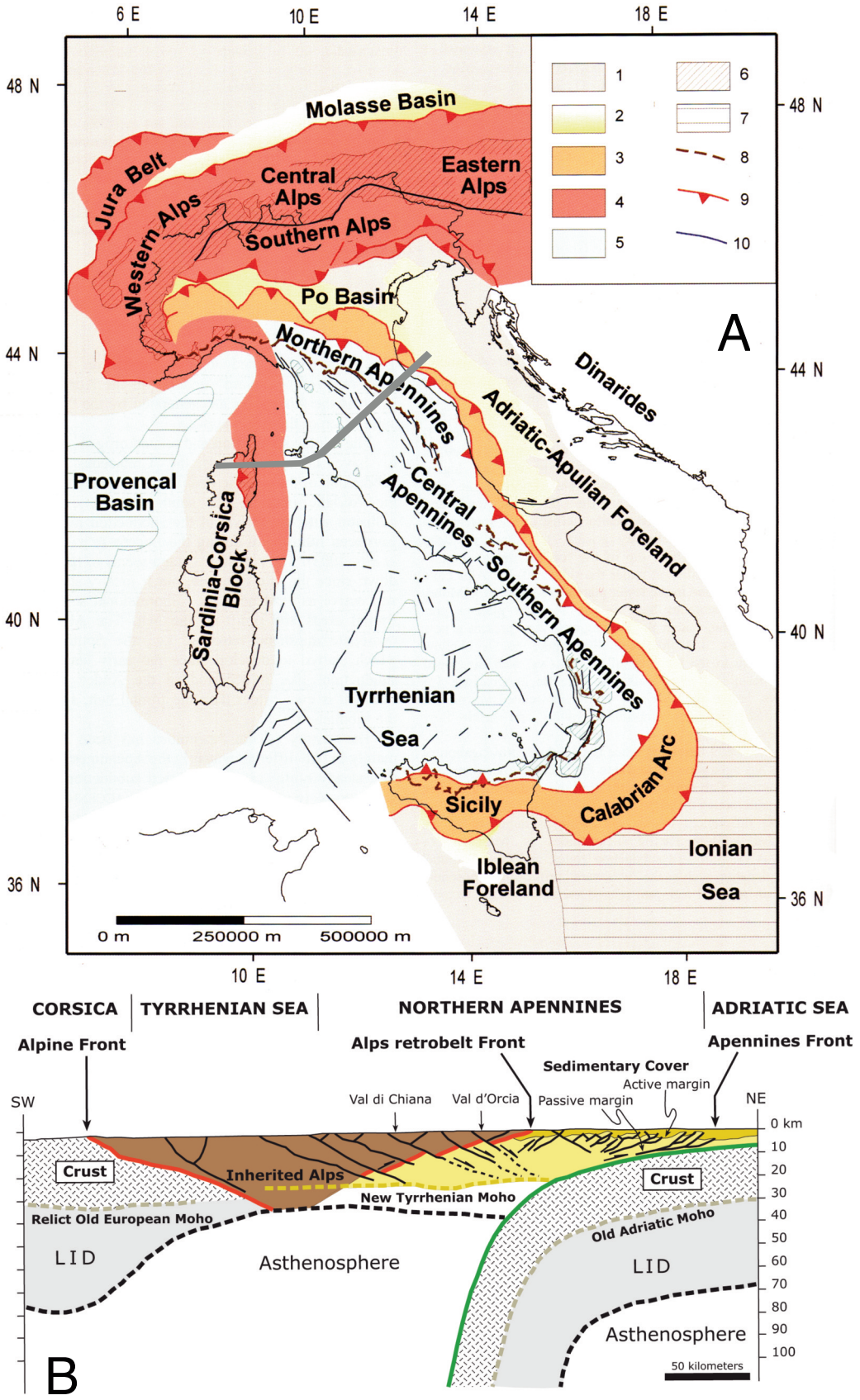

Fig. 2 - A) Synthetic tectonic map of Italy and surrounding regions. 1) foreland areas; 2) foredeep deposits; 3) domains characterized by a compressional tectonic regime in the Apennines; 4) thrust belt units accreted during the Alpine orogenesis; 5) areas affected by extensional tectonics; 6) crystalline basement; 7) areas with oceanic crust; 8) Apennines water divide; 9) thrusts; 10) faults; B) Schematic geological section through the Apennines-Tyrrhenian Sea system. The section trace is shown in A. Modified after Carminati et al. (2004).

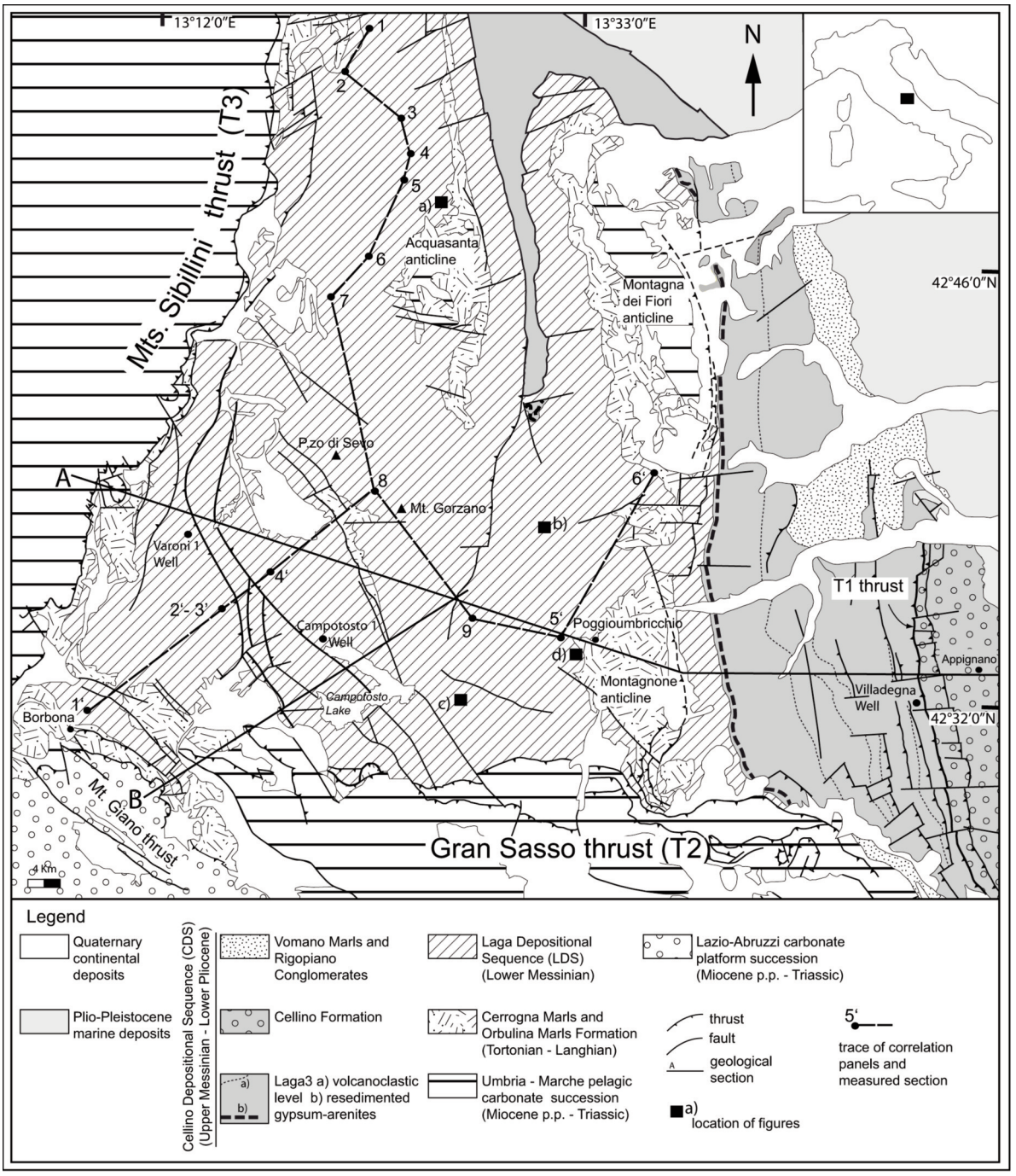

Fig. 3 - a) Geological map of the Laga basin. The dashed lines indicate the trace of the stratigraphic panels of Figs 5 and 6. The continuous lines indicate the trace of the geological sections of Figs 16 and 17. Legend: a, location of the correlation panel of Fig. 9 and of the outcrop of Fig. 10; b, location of the correlation panel of Fig. 7 and the outcrop of Fig. 8; c, location of the outcrop of Fig. 13; d, location of the outcrop of Fig. 14; T1: Teramo thrust. Modified after Centamore et al. (1991).

depositional sequences (Centamore et al., 1991; Centamore and Nisio, 2003 and references therein). The composition of these turbidite deposits indicates as source areas the western and northwestern sectors of the chain, being derived from the erosion of igneous and metamorphic rocks of alpine origin (Chiocchini and Cipriani, 1992) and siliciclastic and carbonate rocks of the same Laga basin substratum (Morelli, 1994; Corda and Morelli, 1996; Valloni et al., 2002). Changes of petrofacies observed from the bottom to the top of the succession were interpreted by the Authors as due to variations in the geographic extension of the catchments system, an element strongly controlled by tectonic activity and climatic changes.

New sedimentological and physical stratigraphic data (77 stratigraphic-sedimentological measured sections for a total thickness of about 11.500 m; Moscatelli, 2003; Milli et al., 2007; Stanzione, 2007; Falcini, 2008, and work in progress), and the integration and re-interpretation of numerous literature data (Centamore et al., 1991, 1992, 1993; Morelli, 1994; Albouy et al., 2003; Artoni, 2003, 2007), allowed to attempt the correlation to the Messinian-Pliocene chronostratigraphic scheme (Iaccarino, 1985; Krijgsman et

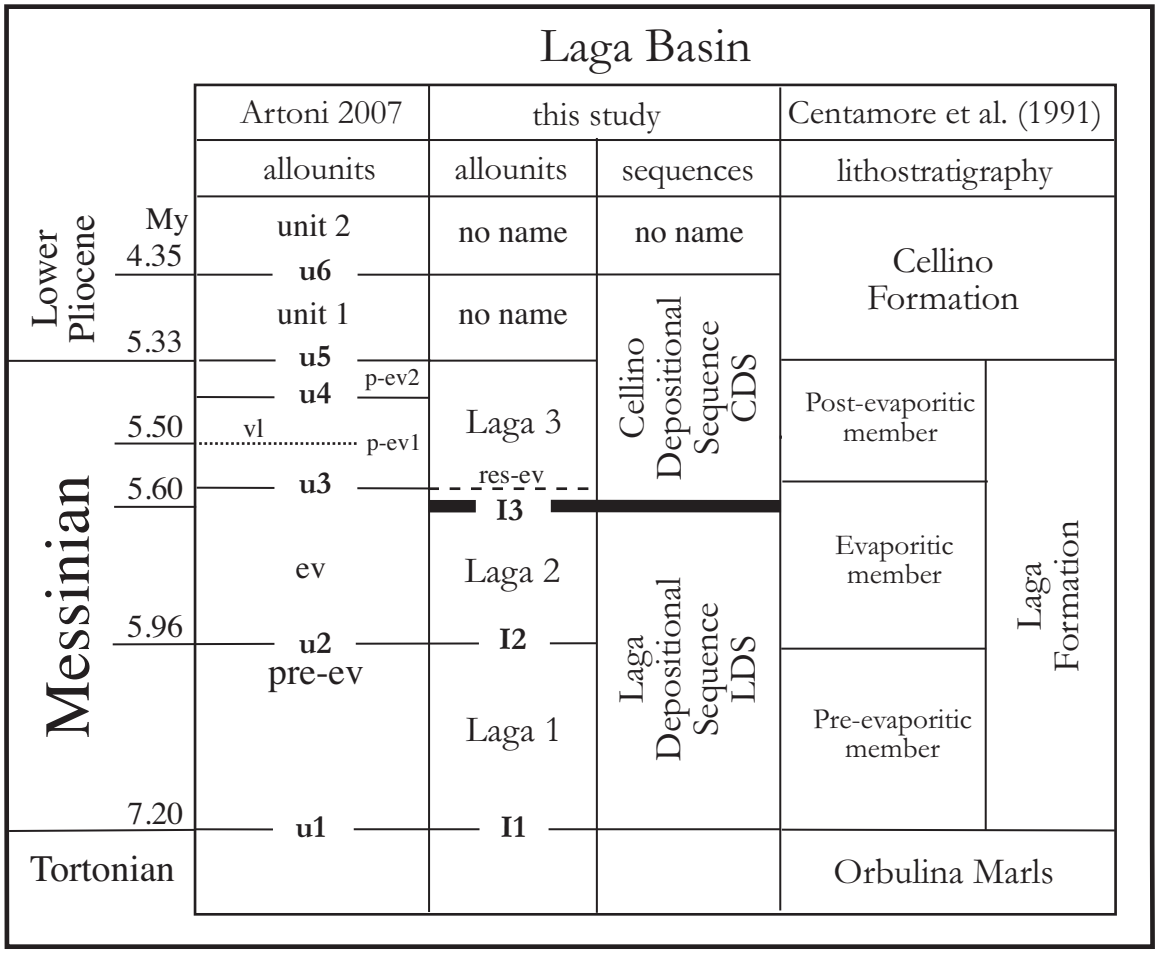

Fig. 4 - Scheme of the main stratigraphic units recognised in the investigated area during the Late Tortonian - Early Pliocene (see text for further explanation). Note that I3 surface is not placed at the base of the resedimented gypsum-arenits, but some hundred meters below, where a change in the evolutional trend between Laga 2 and Laga 3 is recognised. Modified after Milli et al. (2007).

al., 1999a, b; Hilgen et al., 2000; Van Couvering et al., 2000; Roveri et al., 2001; Roveri and Manzi, 2006), and to subdivide the Laga turbidite succession into three main units called Laga 1, Laga 2, and Laga 3, bounded by unconformity surfaces I1, I2, and I3 (Fig. 4). The basin-wide correlations of these units (Figs 5 and 6) and the stratigraphic relationships between the Messinian and the Lower Pliocene deposits have also allowed to date the sedimentation of the Laga 1 during the pre-evaporitic stage (pre-ev) (7.251-5.96 Ma), that of the Laga 2 unit during the evaporitic stage (ev) (5.96-5.61 Ma), and that of the Laga 3 unit during the post-evaporitic stage (p-ev1 and p-ev2) and partially during the lowermost part of the Pliocene (5.61-5.3 Ma; Fig. 4).

Stratigraphic relationships among these units evidence notable thickness variation into the basin. To the west of the Montagna dei Fiori-Montagnone anticline (Fig. 3), Laga 1 and Laga 2 units reach their maximum thickness; it progressively decreases eastward and northward, where the two units onlap onto the substratum. In the same sector the preserved succession of Laga 3 unit is not very thick. To the east of the Montagna dei Fiori-Montagnone anticline, the Laga 1 and Laga 2 units are well located in the subsurface, whereas Laga 3 largely crops out, having a thickness of about 4000 m. It transitionally passes upward and laterally to the mudstone and turbidite deposits of the Vomano Marls Formation and Cellino Formation respectively both of Lower Pliocene in age (Centamore et al., 1992).

The I1, I2, and I3 surfaces have erosive features in the western and proximal sectors of the basin (Sibillini Mts. thrust), and turn into correlative conformities in the distal and eastern sectors, where the passage from Laga 1 to Laga 2, and from Laga 2 to Laga 3 is commonly transitional. The passage from Laga 2 to Laga 3 (I3 surface) constitutes a key point during the Laga basin development as just recognised by previous Authors (Centamore et al., 1991; Artoni, 2003); it marks the first eastward depocenter migration of the Upper Messinian to Present foreland basin system; such migration occurs during the intra-Messinian tectonic phase, an event well recognised in the Apennine foreland basin (see Ricci Lucchi et al., 1982; Ori et al., 1991; Roveri et al., 2001 and references therein). The I3 unconformity represents an important chronostratigraphic surface that both in the Northern Apennine and in Sicily shows evidence of subaerial exposure (Vai, 1988; Grasso et al., 2004; Roveri et al., 2008); it corresponds to the Messinian Erosional Surface (MES), a feature well recognised along the Mediterranean continental margin, being related to deeply incised canyons located in front of the largest river mouths (Ryan and Cita, 1978; Clauzon, 1982; Lofi et al., 2005).

A sequence-stratigraphic framework has been developed for the Laga turbidite succession (Milli et al., 2007) in which two main composite 3rd-order sequences can be recognised. The first sequence, informally named Laga Depositional Sequence (LDS), deposited during the Late

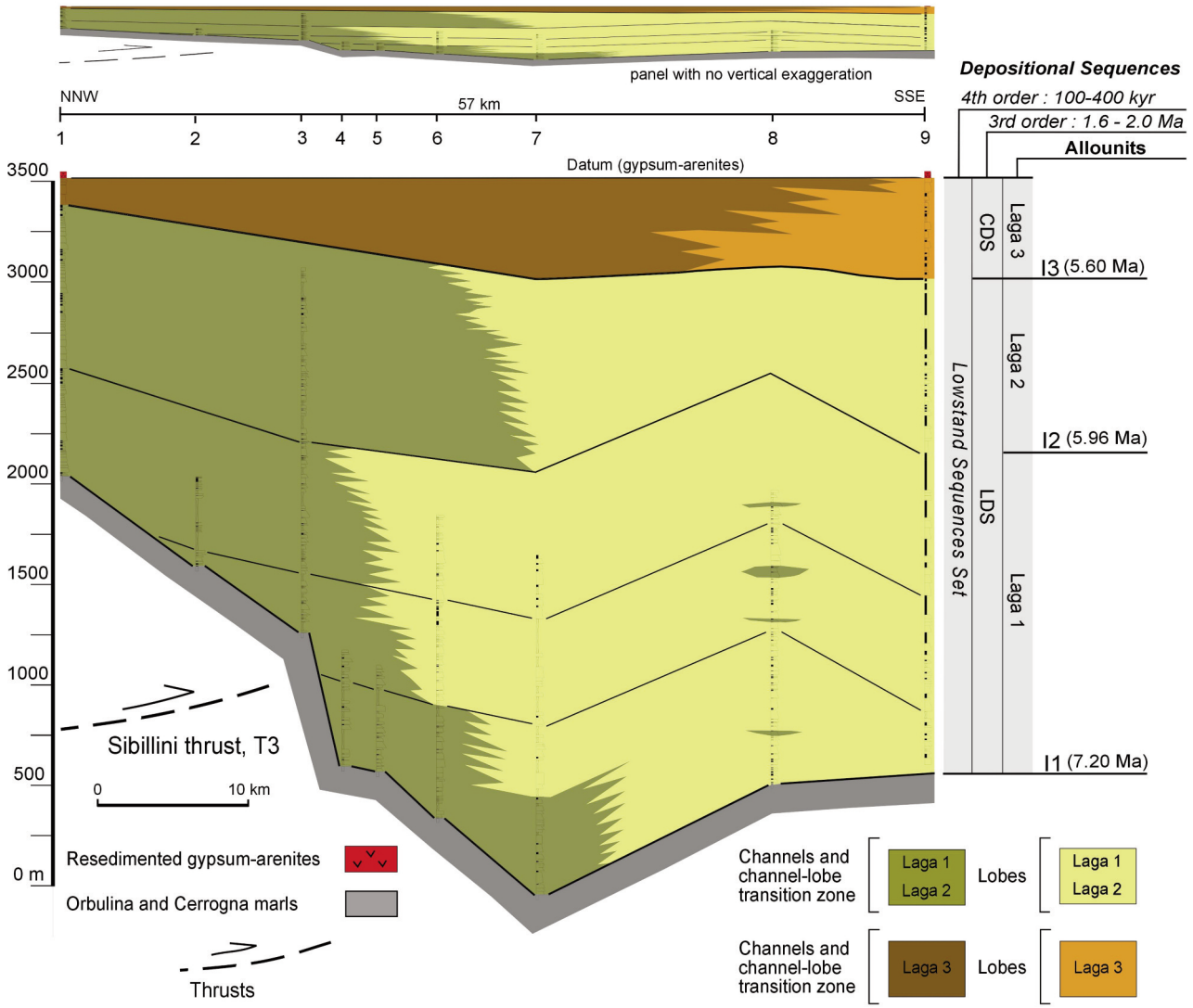

Fig. 5 - NNW-SSE stratigraphic panel of the Laga turbidite deposits. For the trace of panel see Fig. 3. 1) Amandola section; 2) Isola S. Biagio section; 3) Fluvione section; 4) Osoli section; 5) Scalelle section; 6) Acquasanta section; 7) Tronto section; 8) Gorzano section; 9) Vomano section. LDS is Laga Depositional Sequence; CDS is Cellino Depositional Sequence. Modified after Milli et al. (2009).

Tortonian-Early Messinian and comprises the Laga 1 and Laga 2 units; it records the closure phase of the Marnoso-arenacea foreland basin system. The second 3rd-order sequence, informally named Cellino Depositional Sequence (CDS), deposited during the Late Messinian-Early Pliocene and includes the Laga 3 unit, the Vomano marls, and the Cellino Formation (B, C, D, E and F members; see Casnedi, 1976, 1983; Crescenti et al., 1980, 2004; Carruba et al., 2006); it corresponds to the M sequence of Ori et al. (1991), to M2b-P1b sequences of Centamore and Nisio (2003), and to the Lagomare unit and unit1 of Artoni (2007). The upper sequence boundary of the CDS coincides with the u6 surface by Artoni (2007) that has been dated to 4,35 Ma. The Author links the formation of this surface with an important paroxismal tectonic phase that should mark the final reorganization phase of the Cellino turbidite basin. As evidenced by Carruba et al. (2007), such unconformity is well documented in the subsurface by well logs, and it is placed at the base of the A member of the Cellino Formation (Casnedi et al., 1976).

Both of these 3rd-order sequences are interpreted as forming lowstand sequence sets consisting of several 4th-order sequences, which show variable thicknesses ranging from a hundred meters in correspondence of basin margins to several hundred meters in the depocenter sectors. They contain one or more turbidite system, in which channel, channel-lobe transition, and lobe facies have been recognised (Milli et al., 2007, 2009). The general cyclicity characterising these deposits is thought to be controlled by allocyclic processes as pulse of tectonic deformation and/or climatic changes, and by autocyclic processes related to the intrinsic growth of the channel-lobe system (Milli et al., 2007; see also discussion in Mutti and Sonnino, 1981; Beaubouef et al., 1999; Gardner et al., 2003).

ARCHITECTURAL ELEMENTS AND DEPOSITIONAL SETTING OF THE LDS

In this work our analysis is focused on the Laga Depositional Sequence (LDS) because most of the discussed stratigraphic, sedimentological, structural and burial history data are concentrated in this unit. The LDS constitutes a

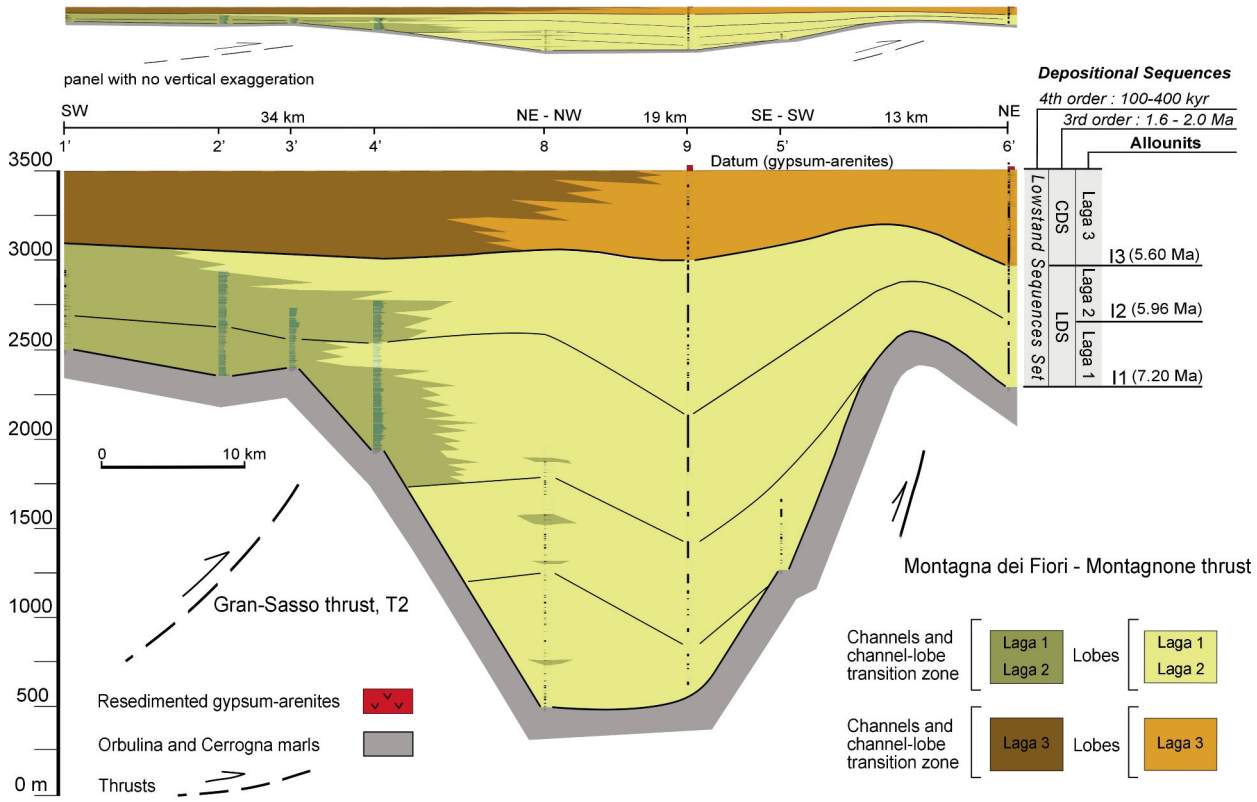

Fig. 6 - SW-NE stratigraphic panel of the Laga turbidite deposits. For the trace of panel see Fig. 3. 1') Borbona section; 2') Varoni well, projected from 0 m to -577 m; 3') Varoni well, projected from -577 m to -923 m; 4') Campotosto well, projected; 8) Gorzano section; 9) Vomano section; 5') Poggioumbricchio section; 6') T. Vezzola section. LDS is Laga Depositional Sequence; CDS is Cellino Depositional Sequence. Modified after Milli et al. (2009).

submarine fan complex where the main architectural elements of a fan, from slope to basin floor passing through the channel sector, can be recognised. The high-frequency sequences forming the LDS (Figs 5 and 6) show a vertical fining- and thinning-upward trend, and contain one or more turbidite system in which it is possible to recognise, from up- to downstream (generally from NW to SE): i) a channel complex zone; ii) a channel-lobe transition zone; and iii) a lobe zone. Downslope and upslope migration of these zones determines, through time, their superimposition and gives rise to a generation of depositional units of different hierarchical order, ranging from meter-thick simple facies sequence to decameters composite facies sequence, expression of single and composite architectural elements as channel and lobe and channel and lobe complexes (see also discussion in Mutti et al., 1994, 1999).

The recognised trend in the high-frequency sequences is interpreted to reflect the deposition during its own early and late lowstand system tracts. In particular the early lowstand system tract (ELST) deposits are essentially constituted by laterally persistent sandstone beds in the medial-distal basin floor (lobe deposits) (Figs 7 and 8) and by the coeval channelized sandy deposits in the proximal portion of the basin. The late lowstand system tract (LLST) deposits consist instead of thin and laterally persistent siltstone and mudstone draping in the basin floor fan and by thick channelized deposits in the proximal sectors (Figs 9 and 10). They record a backstepping of the clastic depositional systems supplying the fan and a protracted period of basin sediment starvation.

Such considerations suggest that during the deposition of the ELST, most of the sands bypassed the channels and deposited as thick and laterally continuous lobes in the medial and distal portion of the fan. Lobes show from up- to downcurrent, three main depositional sub-setting sectors: i) proximal lobe deposits are represented by very thick, lenticular sandstone bodies made up of crudely laminated fine grained sands and locally trough- and cross stratified medium grained sands; ii) distal lobe deposits are constituted by interbedded medium to thick bedded fine to very fine grained sandstones with parallel lamination and traction-plus fall out structures and mudstones; iii) lobe fringe deposits are represented by very fine grained thin bedded turbidites with traction-plus-fall out structures. Slump and debris flow are locally associated to these deposits. Analysis of sandbody geometries and their internal organisation allowed revealing different degree of lenticularity and to hypothesize that depositional topography and, at a larger scale basin physiography, might have controlled the mode of lobe growth (Marini et al., 2009). In the channelized area of the fan erosive features (scours), lag deposits, and thin depositional sandstone bodies consisting of 3D bedforms occurred.

During the LLST most of the sands, instead, deposited into the channels; they formed thick trough-bedded sandstone bodies consisting of 3D bedforms that give rise to composite bars. Lobes of minor thickness and lateral extension occurred in the medial and distal portion of the basin floor fan. At the scale of single facies sequences, both in channel and lobe areas, the recognized fining-upward trend and the more rare coarsening-upward trend can also be the product of local constraints, including channel avulsion, compensation

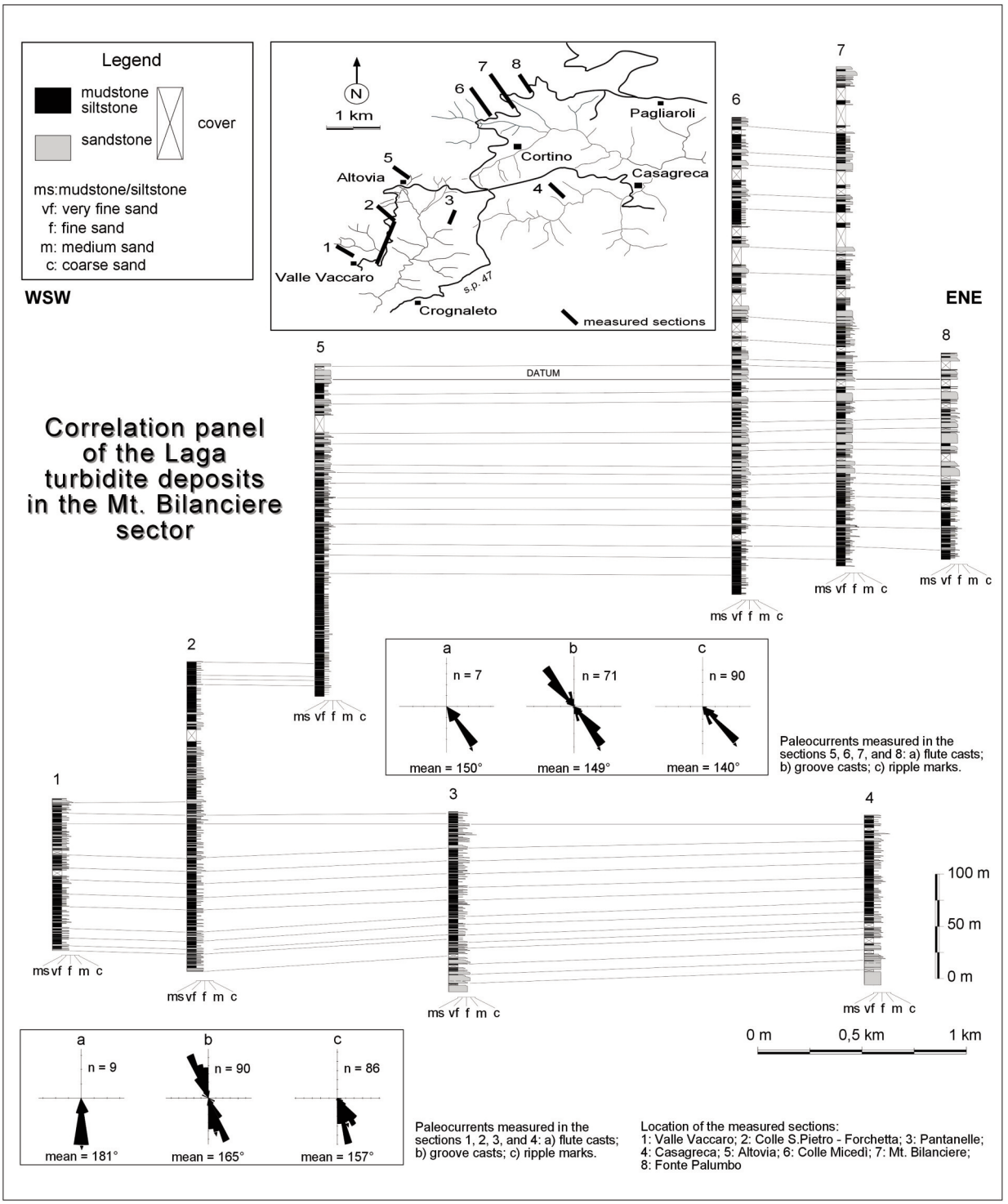

Fig. 7 - Detailed correlation panel of the lobe turbidite deposits in the Mt. Bilanciere sector. Note the high continuity of the sandstone beds in strike section. The correlation panel shows the transitional passage from Laga 1 to Laga 2 units. For location of panel see Fig. 3.

processes, and basin floor topography (Milli et al., 2007, 2009).

The physical features of architectural elements as well as the paleocurrent data, which show a marked change in their direction, from NW-SE in the Laga 1 to N-S in the Laga 2, suggest that basin topography controlled pathway flows, facies and geometry of the channelized and lobes sandstone bodies. The recognised braided geometry of the channelized deposits (Figs 9 and 10), as well as the coarse-medium grain-size and the presence of 3D bedform and composite bars filling the channels (Figs 11 and 12), are features suggesting that against a low gradient of the depositional profile the flows velocity was sufficiently high and consistent with an ondulated seabed promoting a reduced expansion of the flows due to morphological confinement. Likewise, also in the sector where depositional lobes occur, the bodies both in strike and dip section show lenticular and compensation geometries as well as a high abundance of water escape

Fig. 8 - Panoramic view of the Laga 2 sandstone lobes in the M. Bilanciere sector. Paleocurrents towards the observer. For location of outcrop see Fig. 3.

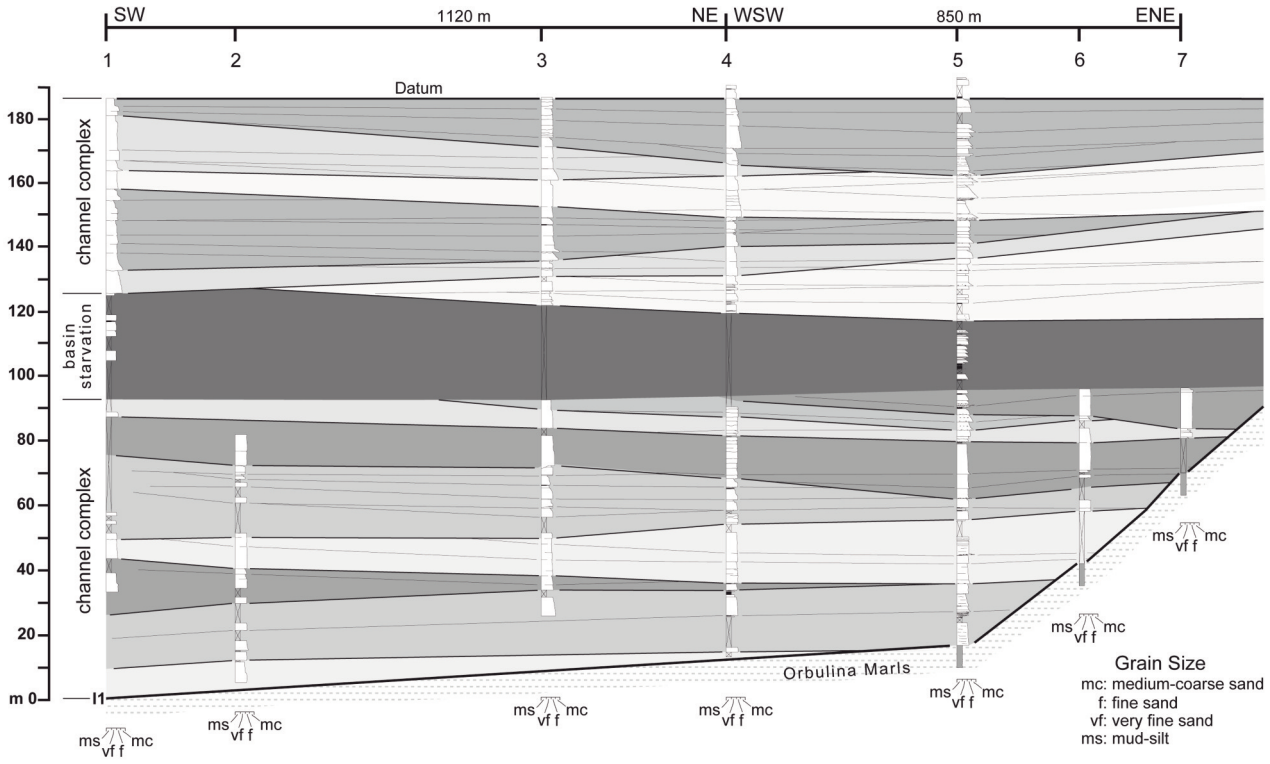

Fig. 9 - Detailed correlation panel showing the channelform hierarchy of the Laga 1 unit. Note the thick fine-grained interval separating the two channel complexes, which record an abandonment phase of the channels and a sediment starvation of the basin. The bodies with different gray tonality indicate composite channels formed by the stacking of single channels (thin lines). For location of outcrop see Fig. 3. After Milli et al.. (2007).

structures consistent with a rapid vertical sediment aggradation during deposition (see discussion in Kneller and Branney, 1995; Baas, 2004; Falcini, 2008; Falcini et al., 2009), a feature that has been interpreted as related to the confinement of the basin and to its own tectonic mobility (see Milli et al., 2009; Tinterri and Muzzi Magalhaes, 2009). Further evidence that the Laga Basin constitutes a confined basin is given by geological map analysis (Fig. 3). A slope opposing to the main flows in the southern sector (Gran Sasso slope) and two lateral slopes in the western (Sibillini thrust) and eastern (Montagna dei Fiori-Montagnone thrust) sectors represented the main topographic elements promoting a rapid deceleration and vertical aggradation of the flows as well as their impact against the slopes, giving rise to reflected and deflected flows with their resulting facies (Fig. 13). This paleogeographic picture is coherent with the delineating geological evolution of this basin during the sedimentation of LDS (Fig. 18). After the involvement of older foredeep deposits in the orogenic wedge, the Laga basin area in which the LDS sedimented was very confined. In fact, it had the thrust front of the orogenic wedge to the west and to the east the outer ramp, a slope coincident with the internal margin of the Montagna dei Fiori-Montagnone thrust on which turbidite onlapped (Fig. 14). The true wedge-top deposits in this sector were the sediments of the Laga 3 unit, passing to the east of Montagna dei Fiori-Montagnone thrust, to the turbidite sediments of the Cellino Formation, which constituted the initial turbidites deposits of the new formed foreland basin system.

Fig. 10 - Channelized sandstone bodies of the Laga 1 unit. Channel fills consist of amalgamated thick-bedded sandstones, which are the expression of migrating three-dimensional bars and bedforms. Channels are characterized by high width/depth ratios and are arranged in laterally offset stacking pattern. Paleocurrents are directed towards the observer (towards SE). For location of outcrop see Fig. 3.

STRUCTURAL SETTING

The Laga basin has been analyzed by seismic lines dataset (both confidential and public), calibrated by bore-hole data (Fig. 3 and 15), in order to reconstruct its structural setting. A 2D seismic dataset comprises seismic profiles that are part of surveys made from 1983-1989, for a total length of about 400 Km. The available well velocity logs of Campotosto 1 Well and Varoni 1 Well (Albouy et al., 2003) allow for the calibrating of seismic lines (Tab. 1). Seismic interpretation was carried out with the recognition of several seismic markers corresponding to (from top to bottom): top of Cerrogna Marls Fm (bottom of the Laga succession, Tortonian), top of Scaglia Rossa Fm. (Eocene), top of Marne a Fucoidi Fm. (Aptian - Albian), top of Calcare Massiccio Fm. (Sinemurian) and the top of Burano Anydrites Fm. (Hettangian). The top of the crystalline basement *s.l.* is located about 3000 m below the top of Burano Anhydrites Fm., using the thickness of the Burano anhydrites and dolostones measured by the well logs in the area (Varoni 1 and Villadegna 1 Wells, Fig. 3). Using the stratigraphy of Varoni 1 well we also distinguish in this interval an upper portion, made of evaporites deposits and a lower portion mainly made of dolostones. This latter is represented with the basement in the cross section of Figs 16 and 17.

Unfortunately, the low quality of the 2D available seismic prevented us from doing a more detailed work of correlation with stratigraphic field data as well as the reconstruction work of strata geometries. Nevertheless, at a larger scale, these data allowed us to reconstruct the trend of the main features of the basin, which are described in two balanced geological cross sections obtained by depth conversion of selected seismic profiles: section A, from the Mts. Sibillini to Appignano village and the section B from Mt. Giano to Mt. Gorzano - Acquasanta anticline (Casero and Bigi, 2006) (Figs 3, 16 and 17).

The observed structural style is characterized by high angle thrust-related-anticlines, trending N-S, with small displacement (hundreds of meters), which progressively decreases from north to south. The main thrust plane recognized in the area is T1 thrust (Fig. 3 and 16). It crops out to the eastern sector of the studied area, and is connected to the more internal and structurally higher Montagna dei Fiori-Montagnone thrust. The hanging wall anticline generated by T1 thrust and the Laga turbidite succession are cut by the Montagna dei Fiori-Montagnone thrust. (Artoni, 2003, 2007; Artoni and Casero, 1997). This geometric relationship suggests that the activity of Montagna dei Fiori-Montagnone thrust is the latest contractional events in the Laga basin. T1 thrust also brings in the hanging wall the Upper Messinian-Lower Pliocene deposits (this latter not included in the section of Fig. 16), and places it onto the turbidites of the Cellino Formation (Lower Pliocene) (Artoni and Casero, 1997; Bigi et al., 1999; Albouy et al., 2003).

As it is shown in Fig. 16, the Laga basin is characterized by a main tectonic transport located at depth along the flat of T1 thrust. At the surface, a smaller displacement can be measured along the same thrust plane on seismic lines (see the gypsum-arenites level as reference in Fig. 16). This progressively upward reduction of the offset suggest that the tectonic activity of T1 was characterized by a variable relationship between propagation and slip on the fault plane, which provided a general uplift of its hanging wall before the deposition of the turbidites deposits of the Cellino Depositional Sequence. During Lower Messinian, the main depocenter of the Laga basin was situated to west of the Montagna dei Fiori-Montagnone anticline; in this sector the onset of T1 thrust activity results to be coeval to the deposition of the Laga 2 unit,which record the general uplift of the western sector. The T1 thrust largely controlled the migration of the Laga basin depocenter from west to east of the Montagna dei Fiori-Montagnone outline, during the deposition of the Laga 3 unit (Upper Messinian) (compare Figs 6 and 16). The east-dipping forelimb of the uplifting anticline in the hanging wall of T1 thrust is well recognizable in all the interpreted seismic lines located along the forelimb of the Montagna dei Fiori-Montagnone thrust. This feature

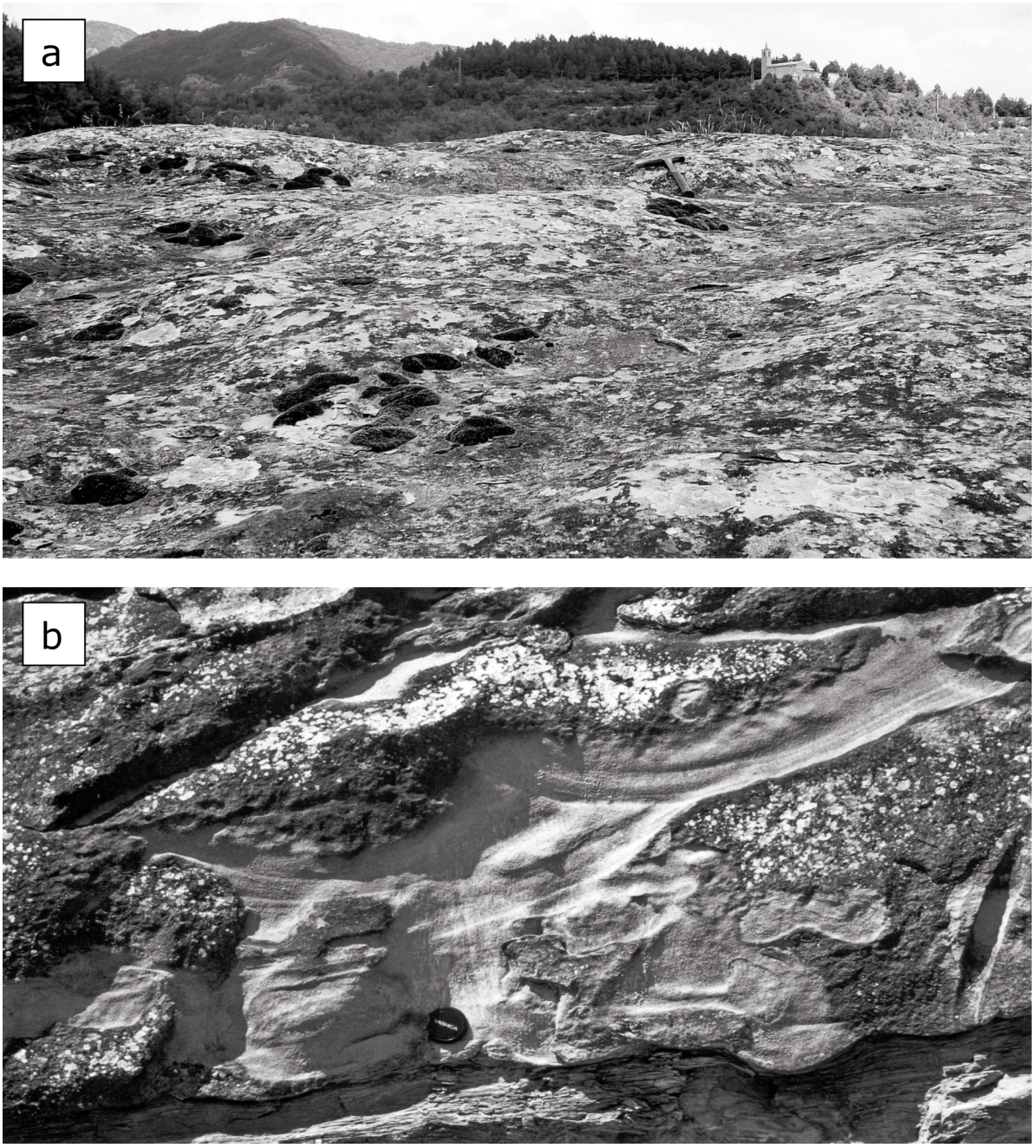

Fig. 11 - a) 3D bedforms with sinuous crestline; b) trough cross-bedding formed by migration of 3D bedforms.

has N-S trend and involved Lower-Upper Messinian deposits. Along this forelimb the Laga 1 and Laga 2 deposits progressively tail off their thickness (Fig. 16).

In the hanging wall of T1 thrust several thrust planes occur, from east to west: the Sibillini Thrust (T3), the Gran Sasso Thrust (T2) and the Acquasanta-Gorzano thrust, recognizable in both the correlation panels (Figs 5 and 6) and geological cross sections (Figs 16 and 17). In the north of the basin, the Acquasanta-Gorzano thrust has N-S trend and the hanging wall anticline has a strong axial culmination in correspondence of Aquasanta village. Following the axial trend to the south, this uplift rapidly decreases along strike, and the thrust passes laterally to a simple anticline in the southern sector, where it is offset by the Gorzano normal fault.

The Gran Sasso thrust (T2) crops out in the south of the Laga basin and is well recognizable in both the cross sections (Figs 16 and 17). It consists of high angle thrust plane, which progressively decreases its offset from south to north (T2 thrust). Moving westward, this E-W trending thrust front progressively changes its trend to N-S, as it can be reconstructed using seismic lines and surface structural trends. In this area, the hanging wall of T2 thrust is constituted by an array of outcropping anticlines and synclines involving the upper part of the Meso-Cenozoic carbonates and the Messinian siliciclastic succession. The result is a structurally complex area composed by thrusts and back-thrusts partially hidden by younger normal faults, which constitutes the footwall of the Sibillini thrust in the north and of Mt.Giano thrust in the south (Fig. 3). T2 thrust

Bar in strike section; flow towards the observer. 3D dunes and ripples constitute the bedforms whose migration and superimposition is strictly related to the passage of the turbidity currents within the channels.

Close-up showing the ondulated crests of the dunes and ripples, giving rise to internal structures often described in literature as festoon or trough cross lamination/bedding.

Geometry and internal stratification of a composite bar in dip section, reconstructed on the base of the field observations.

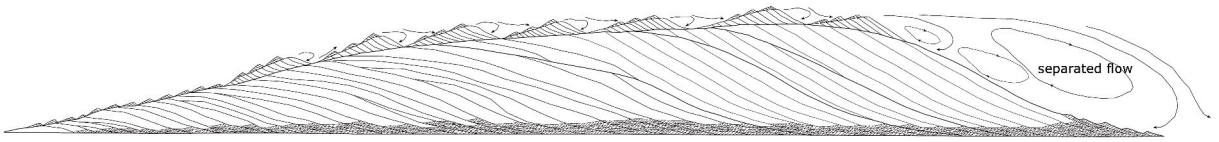

Fig. 12 - Strike and dip section of a composite bar in the channel turbidite deposits of Laga 1 unit.

Fig. 13 - Thick to very thick sandstone beds deposited at the base of the Laga basin frontal slope (Gran Sasso paleoslope, oriented approximately in west-east direction). The great thickness of the beds reflects the rapid sedimentation (aggradation) of the turbidite flows when they approach to the slope. Reflection processes are common in this case and can give rise to facies sequence recording, for the same flow, the sedimentation during the incident (A; red arrows indicate a flow direction towards south) and returning phase (C; yellow arrow indicate a flow direction towards north). B indicates a deposit formed through a rapid sedimentation of the suspended mud; the column of suspended mud can be very high because of the lofting processes (Sparks et al., 1993). For location of outcrop see Fig. 3.

Fig. 14 - Onlap geometry of the Laga 1 unit onto the lower Messinian foreland ramp. Red line indicates the I1 unconformity surface. Gradient of the ramp is estimated at about 6°- 8°(see also Casnedi et al., 2006). The thickness is about 300 m on a length of about 1 km. For location of outcrop see Fig. 3.

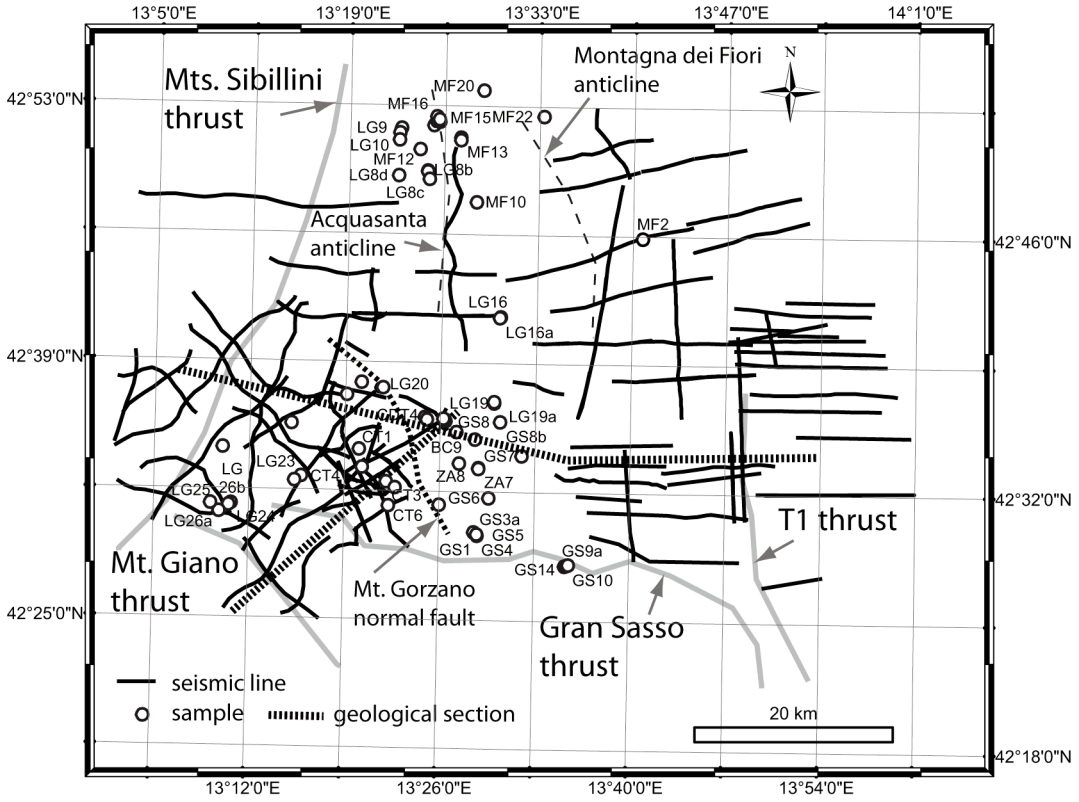

Fig. 15 - 2D seismic dataset used in the area for structural reconstruction. Small circles indicate the location of vitrinite samples.

involved in deformation a reduced thickness of the lower part of the Laga succession (Laga 1 unit, see correlation panels of Figs 5 and 6). As for T1 thrust, correlation of these deposits through the Laga basin testify that Gran Sasso thrust started its activity during deposition of Laga 1 unit. This result assumes an important role in the reconstruction of the basin physiography. This area, structurally located immediately in the footwall of the Sibillini thrust, was the internal slope of the Laga basin during the first stage of Laga 1 deposition, whereas, to the north, the same paleo-geographic position was occupied by the hanging wall of the Sibillini thrust. This evidence also allows correlating coeval turbiditic siliciclastic successions from north to south across the Gran Sasso thrust front itself, and the Messinian turbidites deposits, outcropping to the south, to be considered as the lateral expression of the LDS.

Shortening due to Gran Sasso thrust (T2), Acquasanta-Gorzano thrust and Montagna dei Fiori-Montagnone thrust in the hanging wall of T1 thrust (cross section A) is about 12% (L_0= 57 km and L_1= 50 km), whereas in section B it is about 24% (L_0=31,6 km L_1=24 km). Shortening comprising T1 thrust (section A) is about 18,6% (L_0= 73 km and L_1= 59 km), which means that most of shortening is produced by the T1 thrust in the northern area whereas, moving southward, it can be partly compensated by the Gran Sasso thrust (T2).

The Mt. Gorzano normal fault is crossed by both the geological cross sections A and B (Figs 16 and 17). This fault has a normal offset of about 600 - 800 m and shows a listric geometry. The normal offset is balanced in the sedimentary succession by several back-thrust planes developed in its

Lithological interval	Velocity (m/sec)
Laga Depositional Sequence	3600 m/sec
Top Scaglia F.m-top Cerrogna F.m	4500 m/sec
Top Fucoidi F.m-top Scaglia F.m	5800 m/sec
Top Massiccio F.m–top Fucoidi F.m	6100 m/sec
Top Burano F.m-top Massiccio F.m	6400 m/sec
Burano F.m	6040 m/sec

Tab. 1 - Seismic velocity conversion chart.

hanging wall. As evidenced by interpretation of seismic lines crossing the fault trace, the detachment level of this normal fault can be localized within the Triassic evaporites, whereas its activity is likely due to the extensional phase which follows compression in the Apennines.

PALEO-TEMPERATURE CONSTRAINTS FROM ORGANIC MATTER AND CLAY MINERALOGY PARAMETERS

Materials

Our analysis is based on samples that mainly refer to the Laga 1 and Laga 2 units cropping out to the west of the Montagna dei Fiori-Montagnone anticline (see also Aldega et al., 2007). Thirty six samples for vitrinite reflectance and XRD analyses were collected. Two additional samples pertain to the gypsum arenites of the Laga 3 unit. Pre-orogenic succession was sampled in eight sites in the axial culminations of the main anticlines in the basin (e.g., Montagna dei Fiori area). These deposits belong to the Umbria Marche basinal succession and consist of lithostratigraphic units such as marly limestones containing the organic-rich Bonarelli level (from the Scaglia Bianca Fm., Upper Cretaceous), calcareous marls (from the Rosso Ammonitico Fm., Toarcian-Aalenian), marls (from the Marne a Fucoidi Fm., Aptiani-Albian) and from the Marne con Cerrogna Fm., Tortonian-Langhian). Furthermore, samples from six surface and subsurface (Varoni1 well) sections were analyzed with standardized procedures of Rock Eval pyrolisis (by Elf and discussed in Abouy et al., 2003).

Results-mineralogical data-Pre-orogenic succession

Analyzed samples refer to marls belonging to the Marne con Cerrogna, Marne a Fucoidi and Rosso Ammonitico Fms. (Tab. 2). The Marne con Cerrogna Formation is characterized by illite, illite/smectite mixed layers (I-S), chlorite, kaolinite and non-clay minerals such as quartz, calcite and albite. I-S are R0 structures in which the illite content is in the range 48-50%. Kübler index (KI) data range from 0.89 to 1.01°Δ2θ and from 0.94 to 1.08°Δ2θ in the ethylene glycol solvated and air-dried diffraction patterns respectively (Tab. 2). The Marne a Fucoidi Formation (Aptian-Albian) is mainly composed of illite and I-S in which the smectite component is dominant. The calculated percentage of illite layers in I-S is of 40%. KI values are 1.01 and 1.08°Δ2θ for the ethylene glycol solvated and air-dried oriented mounts, respectively. A slightly different mineral assemblage characterizes the Rosso Ammonitico Formation (Toarcian). Illite, I-S, chlorite and chlorite/smectite mixed layers (C-S) are observed. I-S corresponds to R1 structures with an illitic content of 64%. The Rosso Ammonitico Formation shows KI values of about 1.0-1.1°Δ2θ similar to the overlain deposits.

Results-mineralogical data-Syn-orogenic succession (Laga Depositional Sequence)

Analysis of randomly-oriented whole-rock powder patterns shows that the shales and sandstones of the LDS are composed essentially of quartz, albite, dolomite, calcite, small amounts of K-feldspar and clay minerals. Pyrite, gypsum and gismondine are also identified in a few samples as minor phases.

The < 2 μm grain size fraction in shales and sandstones is

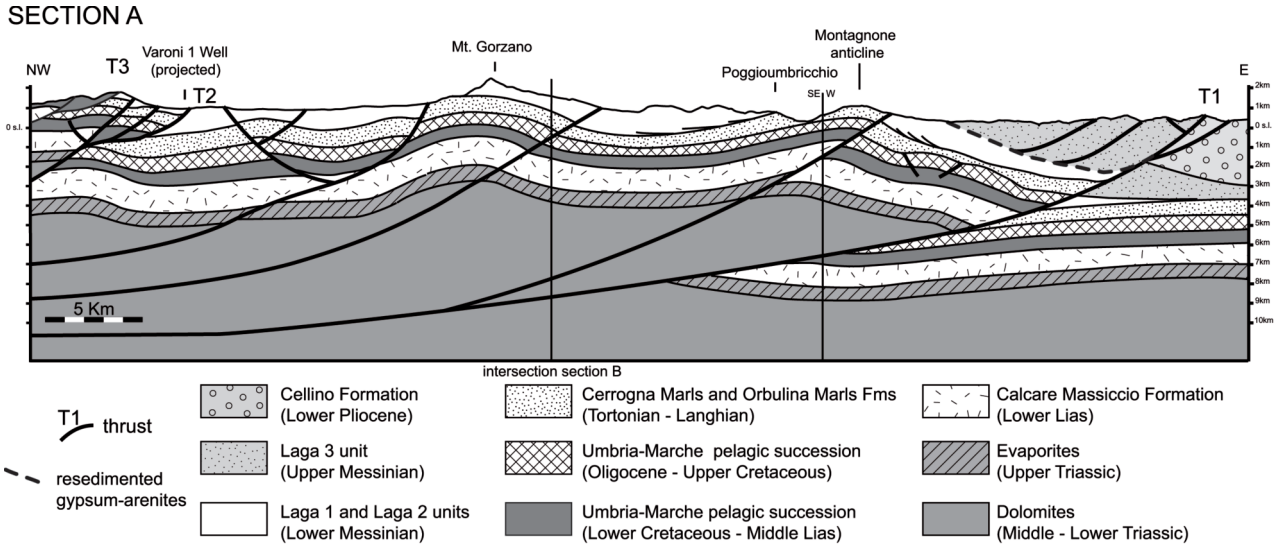

Fig. 16 - Geological section (A) obtained by time to depth conversion of composite 2D seismic lines. For the location of section see Fig. 3.

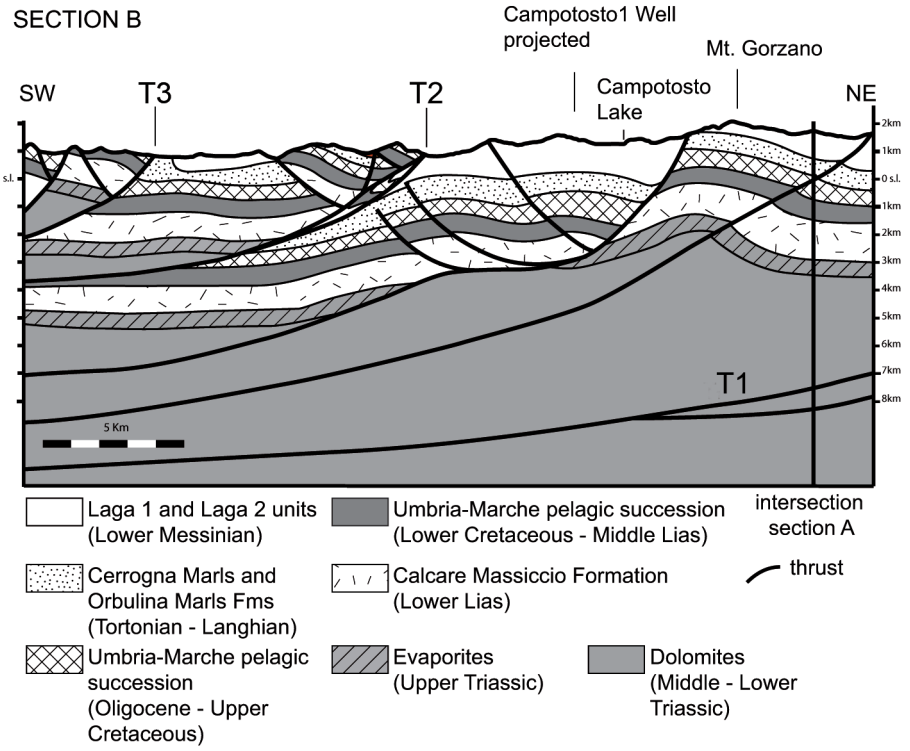

Fig. 17 - Geological cross section (B) obtained by time to depth conversion of composite 2D seismic lines. For the location of section see Fig. 3.

composed mostly of illite, I-S, C-S, kaolinite and chlorite and subordinate non-clay minerals such as quartz, albite, calcite and gismondine. The C-S is mainly restricted to sandstones and its mean composition is C (62%)-S (38%). The I-S shows distinct features in the various lithology associations. The pelitic-arenaceous lithology association displays I-S with random interstratification in which the illitic content is about 50-52%. Three distinct subpopulations of illitic assemblages have been identified in the underlying arenaceous-pelitic lithologies association. They correspond to discrete illite, ordered I-S with smectite layers that do not exceed 25% and disordered I-S with smectite content in the range of 50-52%. In the arenaceous lithology association, only R1 IS were recognized. KI data range from 0.39 to ~ 1.0°Δ2θ in the air-dried specimen, and from 0.34 to 0.84°Δ2θ in the ethylene glycol oriented mounts.

Vitrinite reflectance

Analyses in reflected light provided reliable VRo% values for 30 samples in terms of number of analyzed fragments and measurement distribution (Tab. 2). Data generally show one main cluster identifying the possible autochthonous population of vitrinite-humite macerals. VRo% data indicate immature to early mature stages of hydrocarbon generation with slight differences in the study area.

In the pre-orogenic succession, only one sample provided reliable results from the Bonarelli level comprised almost at the top of the Scaglia bianca Formation (Upper Cretaceous). Several measurements on thermally altered fragments of higher plants indicate a low thermal maturity with VRo of about 0.42%. These components coexist with prevalent fusinite, and both are diluted in abundant amorphous organic matter alternating with pyrite bands. Thus VRo% might be underestimated.

In the LDS analyzed organic matter dispersed in sediments is generally abundant, homogeneous and mainly made up of well-preserved macerals. They belong mainly to the huminite-vitrinite group, with predominant collotelinite and telinite fragments, and subordinate amounts of inertinite group macerals (e.g., fusinite). Pyrite, either finely dispersed or in small globular aggregates, is locally present along the rims of huminite-vitrinite macerals. Data from LDS indicate that the Laga 1 unit shows a range of VRo% between 0.29 and 0.58% indicating immature to early mature stages, whereas the Laga 2 unit is richer in vitrinite fragments and VRo% indicates only the immature stage corresponding to about 0.32%.

Rock-eval data

Rock-eval data (Tab. 3) selected according to Espitalié (1986) derive mainly from the LDS and, subordinately, from the Marne con Cerrogna and Bisciaro Formations (Burdigalian-Lower Tortonian). S1 ranges between 0 and 0.11 mg/g, S2 between 0.25 and 2.64 mg/g, Tmax between 429-443°C, and TOC between 0.51 and 4.62 wt%. Tmax values correlate with immature to early mature and subordinately to middle mature stages of hydrocarbon generation, in agreement with VR% data.

Paleotemperature conversion

To relate the percentage of illite layers in I-S and KI data to maximum paleotemperatures and to the other organic thermal indicators, we adopted the basin maturity chart proposed by Merriman and Frey (1999). The transition from the Early Diagenetic Zone to the Late Diagenetic Zone is marked by 60-80% illite in I-S, KI values of ~1.0°Δ2, VRo = 0.5% and is placed at a temperature of 100°C. At this critical

					KI (°Δ2θ)		XRD analysis	
Sample	**Lithology**	**Rom%±s.d (n. meas.)**	**%I in I-S (R parameter)**	**%C in C-S**	**AD**	**EG**	**<2μm**	**Whole-rock**
Gypsum Arenites (Laga Fm.)								
MF16	shale	0.308±0.039 (100)	N.D.	N.D.	N.D.	N.D.	N.D.	N.D.
MF15	sandstone	0.326±0.05 (102)	N.D.	N.D.	N.D.	N.D.	N.D.	N.D.
Pelitic association (Laga Fm.)								
GS9a	shale	0.459±0.064 (28)	N.D.	N.D.	N.D.	N.D.	N.D.	Qtz8Kfs1Ab13Ph78
GS11	shale	0.473±0.036 (290)	N.D.	N.D.	N.D.	N.D.	N.D.	N.D.
Pelitic-Arenaceous association (Laga Fm.)								
LG19	shale	0.470±0.072 (73)	52 (R0)	N.D.	0.68	0.59	I60I-S18K5Ch17	Qtz8Cal22Ab9Ph50Dol9Py2
PDM5	shale	0.418±0.113 (12)	51 (R0)	N.D.	0.54	0.52	I63I-S6K9Ch22	Qtz8Cal20Kfs1Ab4Ph65Py2
PDM6	shale	0.356±0.136 (10)	52 (R0)	N.D.	0.60	0.54	I62I-S7K7Ch24	Qtz9Cal2Kfs1Ab13Ph75
LG16	sandstone	0.248±0.034 (42)	50 (R0)	62	0.66	0.65	I40I-S14C-S38K3Ch5	Qtz13Cal10Kfs2Ab29Ph39Dol6Py1
LG25	sandstone	0.450±0.029 (59)	50 (R0)	65	0.53	0.50	I52I-S9C-S15Ch24	Qtz21Cal14Kfs2Ab34Ph18Dol11
GS8b	sandstone	0.414±0.034 (15)	N.D.	N.D.	N.D.	N.D.	N.D.	Qtz8Cal17Ab8Ph59Dol6Py
PDM7	sandstone	N.D.	50 (R0)	62	0.52	0.51	I50I-S5C-S20K8Ch17	Qtz22Cal9Kfs1Ab33Ph32Dol3
PDM9	sandstone	N.D.	50 (R0)	65	0.63	0.48	I53I-S9C-S15K7Ch16	Qtz25Cal15Kfs1Ab33Ph23Dol3
Arenaceous-Pelitic association (Laga Fm.)								
CT3	shale	N.D.	50 (R0)	N.D.	0.57	0.54	I70I-S7Ch23	N.D.
CT4	shale	N.D.	74 (R1)	N.D.	0.88	0.71	I56I-S15K8Ch21	N.D.
CSC10	shale	0.579±0.138 (52)	76 (R1)	N.D.	0.70	0.69	I56I-S25K6Ch13	Qtz8Cal18Ab5Ph59Dol6Py4
BC10	shale	0.313±0.087 (19)	50-70 (R0-R1)	62	0.99	0.84	I60I-S24C-S3K3Ch10	Qtz9Cal16Ab8Ph63Dol4
CT2	sandstone	N.D.	N.D.	63	0.54	0.54	I27C-S33K16Ch24	Qtz24Cal15Kfs2Ab42Ph16Dol1
CT5	sandstone	0.419±0.103 (13)	48-73 (R0-R1)	N.D.	0.83	0.64	I50I-S20K12Ch18	Qtz17Cal25Kfs1Ab18Ph34Dol5
CT6	sandstone	0.510±0.040 (9)	73 (R1)	N.D.	0.72	0.64	I37I-S12K6Ch45	Qtz19Cal14Kfs1Ab38Ph22Dol6
CTD4	sandstone	N.D.	50-70 (R0-R1)	66	0.53	0.49	I38I-S6C-S15K16Ch25	Qtz22Cal12Kfs2Ab32Ph26Dol6
CTD3	sandstone	0.488±0.037 (30)	50-70 (R0-R1)	65	0.53	0.49	I36I-S7C-S14K14Ch29	Qtz23Cal15Kfs2Ab33Ph20Dol7
ZAM	sandstone	0.443±0.048 (36)	N.D.	N.D.	N.D.	N.D.	N.D.	N.D.
Arenaceous association (Laga Fm.)								
ZA7	shale	N.D.	66 (R1)	70	0.68	0.51	I59I-S16C-S7K5Ch13	N.D.
ZA8	shale	0.368±0.039 (4)	65 (R1)	70	0.66	0.59	I56I-S10C-S7K8Ch19	Qtz21Cal25Kfs1Ab29Ph21Dol3
LG11	sandstone	0.385±0.027 (40)	N.D.	N.D.	N.D.	N.D.	N.D.	Qtz22Cal2Kfs1Ab50Ph18Dol5Gy2
LG21	sandstone	0.536±0.085 (24)	60 (R1)	57	0.66	0.58	I44I-S15C-S5K9Ch27	Qtz23Cal7Kfs1Ab37Ph26Dol6
LG24	sandstone	N.D.	N.D.	53	0.39	0.34	I30C-S60Ch10	Qtz29Cal19Kfs2Ab35Ph14Dol1
LG26	sandstone	0.474±0.036 (99)	N.D.	N.D.	N.D.	N.D.	N.D.	N.D.
LG27	sandstone	0.365±0.060 (25)	N.D.	40	0.39	0.36	I46C-S40Ch14	Qtz21Cal14Kfs3Ab43Ph14Dol2
MF12	sandstone	0.332±0.099 (44)	N.D.	N.D.	N.D.	N.D.	N.D.	N.D.
MF17	sandstone	0.376±0.054 (11)	N.D.	N.D.	N.D.	N.D.	N.D.	N.D.
MF19	sandstone	0.289±0.047 (102)	N.D.	N.D.	N.D.	N.D.	N.D.	N.D.
MF22	sandstone	0.382±0.057 (9)	N.D.	N.D.	N.D.	N.D.	N.D.	N.D.
GS3	sandstone	0.378±0.031 (20)	N.D.	N.D.	N.D.	N.D.	N.D.	Qtz7Cal22Ab3Ph60Dol6Py2
CT1	sandstone	0.370±0.052 (35)	N.D.	63	0.43	0.43	I28C-S29K10Ch33	Qtz29Kfs1Ab42Ph28
LG8	sandstone	0.398±0.053 (34)	60(R1)	62	0.68	0.59	I55I-S24C-S3K5Ch13	Qtz23Cal3Kfs1Ab16Ph40Dol17
LG10	coal	0.383±0.056 (100)	N.D.	N.D.	N.D.	N.D.	N.D.	N.D.
LG9	coal	0.367±0.028 (31)	N.D.	N.D.	N.D.	N.D.	N.D.	N.D.
Pre-orogenic succession [Marne con Cerrogna (mc), Scaglia Bianca (sb), Marne a Fucoidi (mf), Rosso Ammonitico (ra)]								
MF9	marl (mc)	N.D.	50 (R0)	N.D.	1.03	0.98	I50I-S16K14Ch20	N.D.
MF7	marl (mc)	N.D.	50 (R0)	N.D.	1.07	1.01	I55I-S29K7Ch9	N.D.
MF8	marl (mc)	N.D.	50 (R0)	N.D.	0.99	0.91	I49I-S13K12Ch26	N.D.
MF5	marl (mc)	N.D.	50 (R0)	N.D.	1.08	1.01	I61I-S24K7Ch8	N.D.
MF6	marl (mc)	N.D.	48 (R0)	N.D.	0.94	0.89	I55I-S24K8Ch13	N.D.
MF2	coal (sb)	0.419±0.084 (46)	N.D.	N.D.	N.D.	N.D.	N.D.	N.D.
MF3	marl (mf)	N.D.	40 (R0)	N.D.	1.08	1.01	I59I-S41	N.D.
MF4	marl (ra)	N.D.	64 (R1)	65	1.11	1.03	I66I-S29C-S3Ch2	N.D.

Tab. 2 - Selected organic matter maturity and clay mineralogy data.

Sample	Formation	Thickness (m)*	S1	S2	S3	Tmax	HI	OI	TOC
Borbona West									
AP#15	Laga	430	0.00	0.75	0.47	439	93	58	0.73
Varoni 1 well [Marne con Cerrogna (mc), Bisciaro (bi)]									
161933	mc	-25	0.01	2.33	0.14	438	384	23	0.61
161952	mc	-500	0.06	1.12	0.76	440	200	135	0.56
161954	mc	-550	0.03	0.38	0.10	441	11	3	3.32
161963	bi	-775	0.02	0.25	0.20	443	6	4	4.62
Mt. Gorzano									
AP#23	Laga	50	0.01	0.89	0.28	435	93	58	0.69
AP#24	Laga	105	0.11	2.64	0.84	430	207	66	1.28
AP#25	Laga	149	0.00	0.27	0.36	436	59	79	0.46
AP#26	Laga	242	0.01	1.05	0.92	437	120	106	0.87
AP#34	Laga	1290	0.05	0.82	0.52	430	130	83	0.63
West Acquasanta a & b									
AP#51	Laga	129	0.01	0.43	0.27	434	83	53	0.51
AP#54	Laga	381	0.01	0.35	1.24	437	64	225	0.55
AP#57	Laga	1076	0.01	0.91	0.40	434	142	62	0.64
AP#59	Laga	1195	0.02	1.01	3.33	430	132	43	0.77
Polverina									
POL#06	Laga	340	0.01	0.43	0.27	434	83	53	0.51
POL#12	Laga	521	0.01	0.35	1.24	437	64	225	0.55
POL#21	Laga	1374	0.01	0.43	0.27	434	83	53	0.51
POL#22	Laga	1391	0.01	0.35	1.24	437	64	225	0.55
Leofara									
AP'#74	Laga	129	0.04	2.51	0.59	429	216	50	1.16
AP'#75	Laga	381	0.04	1.93	0.82	435	235	100	0.82
AP'#78	Laga	1076	0.03	0.49	1.01	436	91	188	0.54
AP'#79	Laga	1195	0.03	1.06	0.63	436	126	75	0.84

Notes: Selected Rock-Eval pirolysis data show TOC>0.5, S2>0.3 and S1/S1+S2<0.5
* Thickness calculated from the base of the Laga Formation. Positive values indicate samples for the Laga Fm. Negative values samples for the Marne con Cerrogna and Bisciaro Fms.

Tab. 3 - Rock-eval pirolysis data.

reaction temperature, a major change from random to short-range ordered I-S has been documented by many Authors (Hoffman and Hower, 1979; Srodon, 1999).

Mixed-layer I-S clay minerals become more illitic (up to 95%) within late diagenesis and long-range ordering appears at temperatures of 170-180° C (Hoffman and Hower, 1979; Pollastro 1993). The transition to the anchizone (~200°C) is indexed at KI of 0.42°Δ2θ and associated with vitrinite reflectance values of 2.0% and further reduction in smectite content of I-S. KI values of 0.25°Δ2θ and vitrinite reflectance measurements higher than 4% characterize the transition to the epizone and low-grade metamorphism which occurs at approximately 300°C (Bucher and Frey, 1994). This chart does not consider the reaction progress of trioctahedral phyllosilicates which can be found associated in deeply buried and largely undeformed basinal sedimentary sequences. Usually, C-S mixed layers first appear in diagenesis at temperatures of 60-160°C (Hillier, 1993; Srodon, 1999). Furthermore, to convert vitrinite reflectance data into palaeotemperatures we complemented Merryman and Frey's chart that lacks resolution for VRo values lower than 0.5%, using the equation proposed by Barker and Pawlewicz (1994). It was developed as an empirical calibration based on the assumption that temperature has the dominant influence in increasing VRo% and the effect of heating time is usually on the order of the 'noise' in the experimental determination of VRo% values (Price, 1983; Barker, 1996). This is due to the fact that sampling strategy and outcrop conditions did not offer the opportunity to build refined time-temperature modeling based on both geological and organic maturity inputs (Allen and Allen, 1993).

The identified mixed-layer I-S are random and short-range ordered I-S with a percentage of illite layers ranging from 50 to 76% in Laga samples (Tab. 2). R1 I-S are primarily grouped in a small area to the south of Mt. Gorzano which is part of the depocenter of the basin (Figs 5 and 6). Moving to the west and north, a progressively less severe thermal evolution is recorded; close to the depocenter, both Ro and R1 I-S were recognized in the same samples, whereas only random stacked mixed-layer clays were found at further distances.

Both random and short-range ordered I-S are interpreted as the authigenic phases that have been formed during burial diagenesis since Messinian times. They suggest early diagenetic conditions and associated paleotemperatures between 60-110°C (Hoffman and Hower, 1979; Merriman and Frey, 1999; Srodon, 1999). This is in agreement with the presence of C-S mixed layers of most samples of which the first appearance in diagenesis is generally associated with temperatures of 60 - 160°C (Hillier, 1993). KI-derived temperatures for the Laga succession are higher than those predicted by I-S and C-S. They record late diagenesis or anchizone conditions suggesting temperature ranges of 120-210°C. These values refer to detrital micas inherited from the uplift of the Alpine chain and from rocks eroded in the source areas not directly related to the burial history of the LDS. Thus, KI data cannot be used for the reconstruction of the thermal history of the Laga basin but provide information on provenance and thermal condition of the source rock. In the pre-orogenic succession, KI-derived temperatures approach those calculated from I-S composition. Both parameters are consistent with early and late diagenesis boundary suggesting a maximum temperature not exceeding 100°C. The agreement between temperature-dependent clay mineral parameters and the slow sedimentation rates allow us to state that detrital contribution may have been unimportant for this succession. Paleotemperatures derived from Barker and Pawlewicz's equation (1994) for Laga 1 unit are always lower than 100°C with a mean value of about 60°C irrespective of the stratigraphic position within the pre-evaporitic basin. Lowest values are recorded for the Laga 2 unit with maximum paleotemperatures between 40 and 45°C. On the other hand, data from the pre-orogenic substratum are very scarce and indicate paleotemperatures of about 65°C, probably slightly underestimated because of the presence of amorphous organic matter.

Interpretation of organic matter and clay mineralogy data

We compare calculated maximum burial and the stratigraphic thickness of the LDS between the pre-orogenic substratum and the gypsum-arenites interval (Fig. 18). Loads were calculated from paleotemperatures assuming a pre-erosional geothermal gradient of 22°C/km and a surface temperature of 10°C. Estimated burials based on clay mineralogy in the Lower Messinian depocenter located between Mt. Gorzano and Vomano River range from about 2.2 to 4.0 km and generally agree with measured or extrapolated stratigraphic sections described above (see also Figs 5 and 6).

Moving to the north, available VRo% data indicate a maximum burial of about 1.3-1.6 km in a general agreement with measured stratigraphic thicknesses of about 1.4-2.5 Km. Local anomalies are recorded at the footwall of regional Sibillini and Gran Sasso Thrusts. At the footwall of the Sibillini Thrust, in the Borbona area, the proposed stratigraphic thickness of Laga basin fill varies between 1 and 1.5 km whereas maximum burials higher than 2 km were estimated on the base of either C-S and random I-S coexistence or unoxidised VRo% values between about 0.45 and 0.50%. Thus it seems realistic that this area subdued the thermal imprinting of the presently eroded Sibillini thrust.

In front of the Gran Sasso structure, no complete reconstruction of the sedimentary thicknesses of the LDS is available. Nevertheless, we observe that to the north of Mt. Corvo (western Gran Sasso thrust), VRo% values for the arenaceous lithology association indicate the immature stage of hydrocarbon generation with maximum calculated burials of less than 1.5 km, while to the north of the Corno Grande thrust for the pelitic lithology association, VRo% values indicate the base of the oil window (about 0.5%) with maximum calculated burials of about 2.5 km. Despite samples belonging to different lithology associations, they derive almost all from the base of the Laga Depositional Sequence and from different structural local settings. Sample GS3 belongs to the LDS that probably never experienced any tectonic loading, while GS11 and GS9a samples are from the nucleus of an overturned syncline that represents the footwall of the Corno Grande thrust sheet. This implies that the Gran Sasso thrust localized the displacement in its footwall moving from the west (Borbona area) to the east (Corno Grande area) as already shown by Bigi et al. (1995, 1997) and Speranza et al. (2003).

Low values for the Montagna dei Fiori pre-orogenic succession are indicative of scarce syn-orogenic sedimentary burial mainly represented by the preserved Meso-Cenozoic pre-orogenic succession itself. It is in general agreement with fluid inclusion data from the bottom of the Montagna dei Fiori pre-orogenic succession (Calcare massiccio Formation, Hettangian-Sinemurian). In this unit, homogenization temperatures (Th) are between about 70°C and 90°C due to the maximum sedimentary burial occurred in middle Miocene times and between about 110°C and 130°C due to both hot fluid circulation and sedimentary burial in Late Miocene times (Ronchi et al., 2003).

Further regional studies based on apatite fission tracks and VRo% on the Laga basin were recently performed (Calamita et al., 2004; Rusciadelli et al., 2005; Scisciani and Montefalcone, 2005). They suggest maximum paleo-temperatures ranging between 50°C and 110°C for the Laga succession to the west of the Montagnone-Montagna dei Fiori anticline, in agreement with those proposed in the present study. Nevertheless these maximum paleotemperatures are interpreted as the effect of a ubiquitous and homogeneous tectonic loading due to the emplacement of allochthonous units (Rusciadelli et al., 2005) or thick sedimentary units, now eroded (Scisciani and Montefalcone, 2005). On the other hand, in our hypothesis, variable sedimentary burial due to the Lower Messinian deposits explains our results, except where local anomalies are recorded at the footwall of regional thrust sheets.

TECTONIC EVOLUTION OF THE LAGA BASIN

Our results indicate that between Late Tortonian and Late Messinian, the Laga basin shows the features of a confined basin (Fig. 19) placed at the front of the orogenic wedge and linked up to the outer ramp through the sector of the Montagna dei Fiori-Montagnone anticline, folded during the deposition and then cut, by T1 and T2 thrusts (Fig. 16). Structural, stratigraphic and sedimentological data suggest that the confinement of the basin was product by the thrust propagation into the basin that in turn gave rise to an articulated sea-floor topography (front runner thrust, Allen et al., 1991). The thrust front of the advancing chain raises more external areas of the regional monocline faster than the progressively eastward migration of the monocline itself, and/or that the radius of curvature of the subduction hinge decreases through time. Whatever the cause, the regional

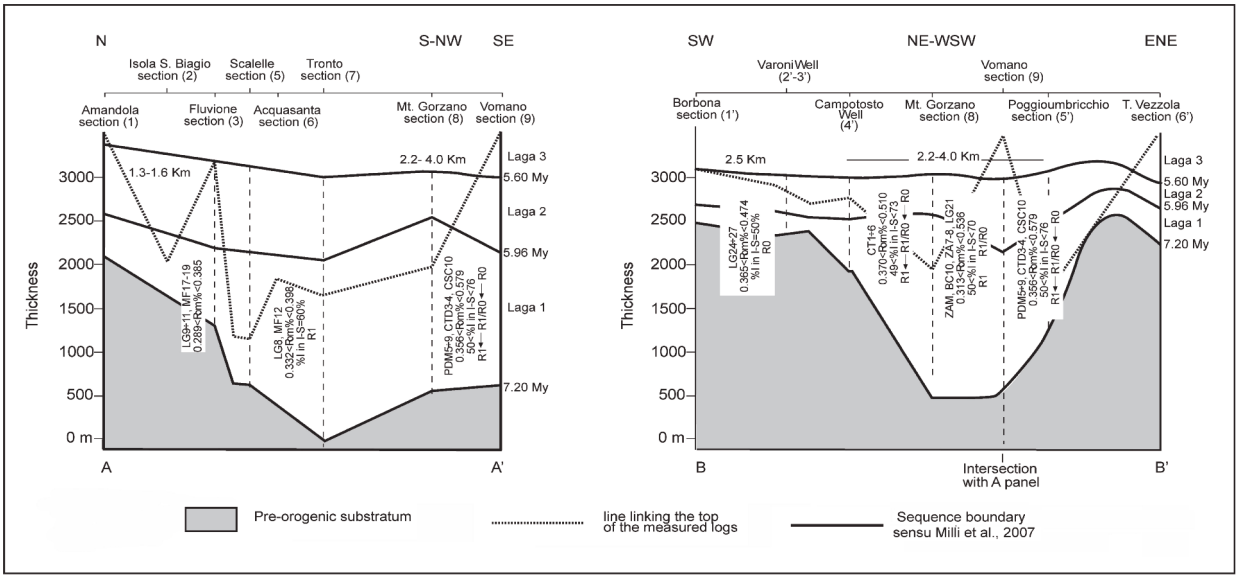

Fig. 18 - Selected organic and inorganic thermal parameters and derived burial values discussed in the text, located onto the correlation panels of Figs 5 and 6 across the Laga basin. Modified after Aldega et al. (2007).

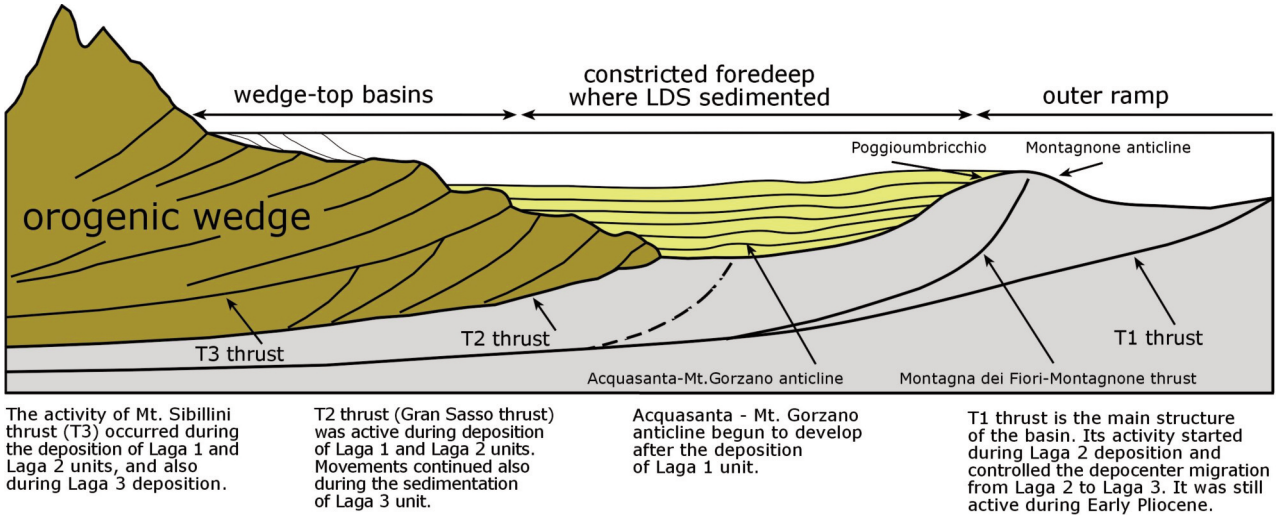

Fig. 19 - a) Schematic cross-section of the foreland basin system at time of sedimentation of LDS. Note as the LDS was depositing in a very constricted and confined foredeep basin situated between the front of the orogenic wedge (front-runner thrust) and the foreland outer ramp.

monocline during the Messinian seems to be generated by a more ancient flexure (Langhian-Serravallian) and is followed by a more external and younger one, starting from Upper Messinian to Lower Pliocene.

The Laga turbiditic deposits record this transitional phase in time and in space. In fact the LDS (lower Messinian) deposited during the propagation of thrusts T1, T2 (Gran Sasso thrust) and T3 (Sibillini thrust). This sequence is representative of the closure of the older Marnoso-Arenacea foreland basin system. The upper Messinian portion (Laga 3 unit), with the younger turbidites deposits of the Cellino Formation (Lower Pliocene), are instead representative of the onset of the present day foreland basin system (Peridriatic basin system, Ori et al., 1991; Centamore et al., 1992).

In particular the sedimentation of Laga 1 unit just occurred in a confined basin showing a more raised sector southwest of Mt. Gorzano, where turbiditic sedimentation insisted on growing anticlines associated to the Gran Sasso thrust (Fig. 3) and a longer and more depressed sector to east of Mt. Gorzano. In the first sector, turbidite systems are smaller and show mostly channelized facies; in the second sector, turbidite systems extend for several tens of kilometers and show a complete development of the architectural elements with the passage from channelized to lobe zones.

The size of the basin and its shape had to be approximately the same as the present-day. Restoration of the two geological cross sections indicates a small shortening value in the hanging wall of T1 thrust, so that the size of the basin was around 75 km wide immediately to the north of the Gran Sasso ridge and about 30-35 km wide around the Acquasanta anticline. The regional monocline, dipping southwestward, was oriented NNW-SSE. It comprises the

eastern limb of the Acquasanta anticline, where the northeastward onlap geometry of the Laga 1 deposits onto the substratum is observable (Fig. 14). The slope-to-basin area was located in correspondence to the present day Sibillini thrust, likely with a N-S trend.

During deposition of Laga 2, the Acquasanta anticline started to grow, folding the described onlap surface and controlling the deposition of sedimentary bodies in the basin. In the Laga 2 unit, turbiditic flows seem to be controlled by the occurrence of growing high to the east and to the south. The differential uplift of the Gran Sasso thrust started to take place: in the southwestern area of the basin, T2 thrust started propagating as far as the associated anticline arrayed at the surface, whereas in the Corno Grande-Mt. Camicia sector, rotation and inversion of the pre-existing structural high took place (Bigi et al., 1997; Calamita et al., 2002). The physiography of the Laga basin during deposition of Laga 2 was partly modified, although geometry of sedimentary bodies strongly suggests that no migration of the system occurred (Figs 5 and 6). The I2 surface at the base of the Laga 2 can in fact be interpreted as the expression of a local intrabasinal shift of depocenter, controlled by the thrust activity (Artoni, 2003; Milli et al., 2007). At the end of the Laga 2 deposition, the basin was completely overfilled, and the whole area started to uplift. This process can be due to the propagation of the T1 thrust. The I3 surface, located between Laga 2 and Laga 3, represents the depocenter shift from the west to the east of the Montagna dei Fiori-Montagnone ridge (Figs 6 and 16). The western area was uplifted and tectonically transported, as well as the Gran Sasso Ridge, to the south. These structures occurred in the hanging wall of the T1 thrust, which controlled the new morphology of the basin. The growing T1 thrust hanging wall anticline produced an internal slope of the basin, which separated a higher internal sector of the basin, site of channel and channel-lobe transition turbidites sedimentation, from an external deeper sector where basin plain turbidite sedimentation occurred (Centamore et al., 1993; Milli et al., in progess). This morphological configuration should be representative of the inner foredeep sector related to the new and more eastern foreland basin systems formed in connection with the intra-Messinin tectonic phase. T1 thrust continued to propagate cutting even the CDS, which is passively transported on top of the thrust over the Cellino Formation during the Lower Pliocene time. This younger activity of T1 is coeval to the reactivation of the Montagna dei Fiori thrust which propagates in the T1 hanging wall and cut all the previous structures (Fig. 16).

CONCLUSION

In this paper we presented an integrated methodological approach to the study of the Messinian Laga Basin recording the passage from two different foreland basin systems. This approach takes into account: i) physical and sedimentological data providing correlation across the basin, pieces of information on basin physiography and localization of the source areas; ii) interpretation of the available seismic dataset, providing reconstruction of structural style and evaluation of the shortening in Neogene time; iii) thermal maturity data of organic matter dispersed in sediments and clay mineralogy analyses providing pieces of information on the sedimentary and/or tectonic burial of the turbidite succession. The results indicate that the Lower Messinian Laga Basin constitutes a confined basin placed at the base of orogenic wedge, which marked the passage to the Upper Miocene to Present foreland basin system. The observed migration of local depocenters in the Laga Basin and the passage to the new foreland basin system is strictly controlled by thrust activity that, together with climate changes, exerted a major control on sediment supply and on stratigraphic organization of this sedimentary succession.

The advancing orogenic wedge raised the external areas of the regional monocline faster than the progressively eastward migration of the monocline itself, and/or than the decreasing of curvature radius of the subduction hinge through time. Thrusting migrates progressively eastward and the orogenic wedge is actively deformed, but the foreland basin system does not migrate, and no new accommodation space formed in front of the deformed chain (see also Ford, 2004). This is confirmed by the sedimentological characters of the LDS indicating a deposition into a constricted and confined foredeep basin having a sea-floor topography being the result of front-runner thrusts propagation.

The total shortening of the Laga basin obtained by the restoration of two geological cross section across the basin is about 20% and indicates that the basin size is almost preserved. The burial history, based on organic matter and clay mineralogy parameters (Fig. 18 and Tab. 2), is essentially due to the sedimentary load of Laga 1-Laga 2 sequences in the western part of the basin. Maximum temperature values in the Laga succession are reached close to the main thrust front, due to additional tectonic burial.

The presented data strongly suggests that the Laga basin where LDS sedimented, can be described as an internally deformed but not migrating orogenic wedge, developed during Messinian time in the Central Apennines (Fig. 19). At the same time this also entails that the regional monocline should be generated by a more ancient flexure (Langhian-Serravallian) corresponding to the more internal and ancient foredeep basin, filled by the Marnoso Arenacea Formation. As such the Laga basin where LDS sedimented can be interpreted as the closure phase of the Marnoso arenacea foreland basin system, having features recording the transition from two different foreland basin systems.

ACKNOWLEDGMENTS - This study is the result of a strict collaboration between the Authors. An initial version of the manuscript was read by R. Butler and F. Roure whose comments and constructive criticism were utilized to improve the text. Several people are also thanked for the discussion on evolution of the Laga Basin: E. Centamore, E. Mutti, F. Ricci Lucchi, S. Lugli, V. Manzi, M. Roveri, R. Ravnas, C. Guargena, and C. Doglioni. We also thank A. Artoni and W. Paltrinieri for the careful and detailed revision of the manuscript. Financial support was provided by NorkeShell and StatoilHydro and by SAPIENZA, Università di Roma.

REFERENCES

Albouy E., Casero P., Eschard R., Rudkiewicz J.L., Sassi W. 2003. Coupled structural/stratigraphic forward modeling in the Central Apennines. In: Proceedings, American Association of Petroleum Geologists, Annual Convention: 11-14 May, Salt Lake City, Utah.

Aldega L., Botti F., Corrado S. 2007. Clay mineral assemblages and vitrinite reflectance in the Laga Basin (Central Apennines Italy): what do they record? Clay and Clay Minerals: 55, 504-518.

Allen P.A., Allen R.R. 1993. Basin Analysis Principles and Applications. Oxford, Blackwell, 451 pp.

Allen P.A., Homewood P. 1986. Foreland basins. International Association of Sedimentologists, Special Publication: 8, 453 pp.

Allen P.A., Crampton S.L., Sinclair H.D. 1991. The inceptionand earlyevolution of the North Alpine Foreland Basin, Switzerland. Basin Research: 3, 143-163.

Argnani A., Ricci Lucchi F. 2001. Tertiary siliciclastic turbidite systems of the Northern Apennines. In: Vai G.B., Martini I.P., (Eds.), Anatomy of an Orogen: the Apennines and Adjacent Mediterranean Basins. Kluwer Academic Publishers, 327-350.

Artoni A. 2003. Messinian events within the tectono-stratigraphic evolution of the Southern Laga Basin (Central Apennines, Italy). Bollettino della Società Geologica Italiana: 122, 447-465.

Artoni A. 2007. Growth rates and two-mode accretion in the outer orogenic wedgw-foreland basin system of Central Apennine (Italy). Bollettino della Società Geologica Italiana: 126, 531-556.

Artoni A., Casero P. 1997. Sequential balancing of growth structures, the late Tertiary example from the Central Apennine. Bulletin Société Géologique France: 168, 35-49.

Artoni A., Di Biase D., Mutti E., Tinterri R. 2000. Control of thrust propagation on turbidite sedimentation. EAGE Conference on geology and petroleum geology of the mediterranean and circum-mediterranean basins. Malta, Extended abstrats book, C21.

Baas J.H. 2004. Conditions for formation of massive turbiditic sandstones by primary depositional processes. Sedimentary Geology: 166, 293-310.

Bally B.W., Burbi L., Cooper C., Ghelardoni R. 1986. Balanced sections and seismic reflection profiles across the Central Apennines. Memorie della Società Geologica Italiana: 35, 257–310.

Barker C. 1996. Thermal modeling of petroleum generation: theory and applications. Amsterdam, Elsevier, 512 pp.

Barker C.E., Pawlewicz M.J. 1994. Calculation of vitrinite reflectance from thermal histories and peak temperatures. A comparison of methods. In: Mukhopadhyay P.K., Dow W.G., (Eds.), Vitrinite reflectance as a maturity parameter: applications and limitations: ACS Symposium Series, 570, 216-229.

Beaubouef R.T., Rossen C., Zelt F.B., Sullivan D.C., Mohrig D.C., Jennette D.C. 1999. Deep-water sandstones, Brushy Canyon Formation, west Texas. Field Guide for AAPG Hedberg Field Research Conference, April 15-20, 1999. AAPG Continuing Education Course Note Series: 40.

Beaumont C. 1981. Foreland basin. Geophysical Journal of the Royal Astronomical Society: 65, 291-329.

Bigi S., Costa Pisani P. 2005. From a deformed Peri-Tethyan carbonate platform to a fold-and-thrust-belt: an example from the Central Apennines (Italy). Journal of Structural Geology: 27, 523–539.

Bigi S., Calamita F., Paltrinieri W. 1995. Modi e tempi della strutturazione della catena appenninica abruzzese dal Gran Sasso alla costa adriatica. Studi Geologici Camerti: volume speciale 1995/2, 77-85.

Bigi S., Cantalamessa G., Centamore E., Didaskalou P., Micarelli A., Nisio S., Pennesi T., Potetti M. 1997. The periadriatic basin (Marche-Abruzzi sector, Central Italy) during the Plio-Pleistocene. Giornale di Geologia: 59, 245-259.

Bigi S., Calamita F., Cello G., Centamore E., Deiana G., Paltrinieri W., Pierantoni P.P., Ridolfi M. 1999. Tectonics and sedimentation within a Messinian foredeep in the Central Apennines, Italy. Journal of Petroleum Geology: 22, 5-18.

Bigi S., Costa Pisani P., Milli S., Moscatelli M. 2003. The control exerted by pre-thrusting normal faults on the Early Messinian foredeep evolution, structural styles and shortening in the Central Apennines (Lazio-Abruzzo area, Italy). Studi Geologici Camerti: num. spec. 2003, 17-37.

Boccaletti M., Ciaranfi N., Cosentino D., Deiana G., Gelati R., Lentini F., Massari F., Moratti G., Pescatore T., Ricci Lucchi F., Tortorici L. 1990. Palinspastic restoration and paleogeographic reconstruction of the peri-Tyrrenian area during the Neogene. Paleogeography Paleoclimatology Paleoecology: 77, 41-50.

Bucher K., Frey M. 1994. Petrogenesis of metamorphic rocks. Springer-Verlag, Berlin, 318 pp.

Calamita F., Cello G., Centamore E., Deiana G., Micarelli A., Paltrinieri W., Ridolfi M. 1991. Stile deformativo e cronologia della deformazione lungo tre sezioni bilanciate dall'Appennino umbro-marchigiano alla costa adriatica. Studi Geologici Camerti: vol. spec. 1991/1, 295-314.

Calamita F., Viandante M.G., Hegarty K. 2004. Pliocene-Quaternary burial-exhumation paths in the Central Apennines (Italy): implications for the definition of the deep structure of the belt. Bollettino della Società Geologica Italiana: 123, 503–512.

Carminati E., Doglioni C., Scrocca D. 2004. Alps Vs Apennines. In: Crescenti U., D'Offizi S., Merlino S. and Sacchi L., (Eds.) Geology of Italy: Special Publication of the Italian Geological Society for the IGC 32nd. Florence, 2004, 141-151.

Calamita F., Scisciani V., Adamoli L., Ben M'Barek M., Pelorosso M. 2002. Il sistema a thrust del Gran sasso (Appennino centrale) Studi Geologici Camerti: nuova serie 1/2002, 19-32.

Carruba S., Casnedi R., Felletti F. 2007. Sedimentary evolution in a migrating foredeep basin: geometry and facies analysis if the massive sandy bodies of the Cellino Formation, Lower Pliocene Periadriatic foredeep (Central Apennines, Italy). Bollettino della Società Geologica Italiana: 123, 503–512.

Carruba S., Casnedi R., Perotti C.R., Tornaghi M., Bolis G. 2006. Tectonic and sedimentary evolution of the Lower Pliocene Periadriatic foredeep in central Italy. International Journal of Earth Sciences (Geol. Rundsch.): 95, 665-683.

Casero P. 2004. Structural setting of petroleum exploration plays in Italy. In: Crescenti U., D'Offizi S., Merlino S., Sacchi L. (Eds.), Geology of Italy. Special Publication of the Italian Geological Society for the IGC 32nd. Florence, 2004, 189-199.

Casero P., Bigi S. 2006. Deep structure of the Laga Basin. European Geophysical Union General Assembly, Abstract and Programs, TS7.2XY0591.

Casnedi R. 1976. Analisi sedimentologica di torbiditi del sottosuolo abruzzese con i carotaggi elettrici. Atti Istituto di Geologia Università di Pavia: 26, 48-55.

Casnedi R. 1983. Hydrocarbon-bearing submarine fan system of Cellino Formation, central Italy. American Association of Petroleum Geologists Bulletin: 67, 359-370.

Casnedi R., Follador U., Moruzzi G. 1976. Geologia del campo gassifero di Cellino (Abruzzo). Bollettino della Società Geologica Italiana: 95, 891-901.

Casnedi R., Ghielmi M., Rossi M., Cazzola L., Serafini G. 2006. Geometrical analysis and seismic modelling of an outer foredeep margin in the lower Messinian Laga turbidite complex (Central Apennines, Abruzzo, Italy). Bollettino della Società Geologica Italiana: 125, 203-220.

Centamore E., Nisio S. 2003. Significative events in the Periadriatic foredeeps evolution (Abruzzo-Italy). Studi Geologici Camerti: num. spec. 2003, 39-48.

Centamore E., Bigi S., Berti D., Micarelli A., Morelli C. 1992. Nuovi dati sui depositi neogenici di avanfossa del pescarese. Bollettino della Società Geologica Italiana: 111, 437-447.

Centamore E., Cantalamessa G., Micarelli A., Potetti M., Berti D., Bigi S., Morelli C., Ridolfi M. 1991. Stratigrafia e analisi di facies dei depositi del Miocene e del Pliocene inferiore dell'avanfossa marchigiano-abruzzese e delle zone limitrofe. Studi Geologici Camerti: 1991/2, 125-131.

Centamore E., Cantalamessa G., Micarelli A., Potetti M., Ridolfi M., Cristallini C., Morelli C. 1993. Contributo alla conoscenza dei depositi terrigeni neogenici di avanfossa del teramano (Abruzzo settentrionale). Bollettino della Società Geologica Italiana: 112, 63-81.

Chiocchini U., Cipriani N. 1992. Provenance and evolution of Miocene turbidite sedimentation in the Central Apennines. Sedimentary Geology: 77, 185-195.

Cipollari P., Cosentino D. 1995. Miocene unconformities in the Central Apennines: geodynamic significance and sedimentary basin evolution. Tectonophysics: 252, 375-389.

Clauzon G. 1982. Le canyon messinien du Rhone: une preuve decisive du desiccated deep-basin model [Hsü, Cita et Ryan, 1973]. Bulletin Societé Geologique du France: 24, 597-610.

Corda L., Morelli C. 1996. Compositional evolution of the Laga and Cellino sandstones (Messinian-Lower Pliocene, Adriatic foredeep). Bollettino della Società Geologica Italiana: 115, 423-437.

Corrado S. 1995. Nuovi vincoli geometrico-cinematici all'evoluzione neogenica del tratto meridionale della linea Olevano-Antrodoco. Bollettino della Società Geologica Italiana: 114, 245-276.

Corrado S., Miccadei E., Parotto M., Salvini F. 1995. Evoluzione tettonica del settore di Montagna Grande (Appennino centrale): il contributo di nuovi dati geometrici, cinematici e paleo-geotermici. Bollettino della Società Geologica Italiana: 114, 325-338.

Crescenti U., D'Amato C., Balduzzi A., Tonna M. 1980. Il Plio-Pleistocene del sottosuolo abruzzese-marchigiano tra Ascoli Piceno e Pescara. Geologica Romana: 19, 63-84.

Crescenti U., Milia M.L., Rusciadelli G. 2004. Stratigraphic and tectonic evolution of the Pliocene Abruzzi basin (Central Apennines, Italy). Bollettino della Società Geologica Italiana: 123, 163-173.

De Celles P.G., Giles K.A. 1996. Foreland basin systems. Basin Research: 8, 105-123.

Doglioni C., Carminati E., Cuffaro M. 2006. Simple kinematics of subduction zones: International Geological Review: 48, 479-493.

Espitalié J. 1986. Use of Tmax as a maturation index for different types of organic matter. Comparison with vitrinite reflectance. In: Burrus J. (Ed.), Thermal modeling in sedimentary basins. Paris, Editions Technip, 475-496.

Falcini F. 2008. Analytical modelling of turbidity currents: inferring of paleo-flow conditions from turbidites deposits (an example for the Laga Basin, central Apennines, Italy). Ph.D Thesis, SAPIENZA Università di Roma, 109 pp.

Falcini F., Marini M., Milli S., Moscatelli M. in press. An inverse problem to infer paleoflow conditions from turbidites. Journal of Geophysical Research, doi:10.1029/2009JC005294.

Flemings P.B., Jordan T.E. 1990. A synthetic stratigraphic model of foreland basin development. Journal of Geophysical Research: 94, 3851-3866.

Ford M. 2004. Depositional wedge tops: interaction between low basal friction external orogenic wedges and flexural foreland basins. Basin Research: 16, 361-375.

Gardner M.H., Borer J.M., Melick J.J., Mavilla N., Dechense M., Wagerle R.N. 2003. Stratigraphic process-response model for submarine channels and related features from studies of Permian Brushy Canyon outcrops, West Texas. Marine and Petroleum Geology: 20, 757-787.

Ghisetti F., Vezzani L. 1997. Interfering paths of deformation and development of arcs in the fold-and-thrust belt of the Central Apennines (Italy). Tectonics: 16, 523-536.

Ghisetti F., Barchi M., Bally A.W., Moretti I., Vezzani L. 1993. Conflicting balanced structural sections across the Central Apennines (Italy): problems and applications. In: Spencer A.M. (Ed.), Generation, accumulation and production of european hydrocarbons III. European Association Petroleum Geology, Special publication: 3, 219-231, Springer-Verlag, Heidelberg.

Grasso M., Butler R.W.H., Schmincke H.U. 2004. The Neogene thrust-top basins incentral Sicily and the Neogene volcanism of the Northern Monti Iblei. B30 Field trip guidebook 32nd International Geological Congress, Florence, 2004.

Hilgen F.J., Iaccarino S., Krijgsman W., Villa G., Langereis C.G., Zachariasse W.J. 2000. The Global Boundary Stratotype Section and Point (GSSP) of the Messinian Stage (uppermost Miocene). Episodes: 23, 172-178.

Hillier S. 1993. Origin, diagenesis, and mineralogy of chlorite minerals in Devonian lacustrine mudrocks, Orcadian Basin, Scotland. Clays and Clay Minerals: 41, 240-259.

Hoffman J., Hower J. 1979. Clay mineral assemblages as low grade metamorphic geothermometers: applications to the thrust faulted disturbed belt of Montana, USA. In: Scholle P.A, Schluger P.R. (Eds.), Aspect of diagenesis. SEPM (Society for Sedimentary Geology) Special Publication: 26, 55-79.

Iaccarino S. 1985. Mediterranean Miocene and Pliocene planktic foraminifera. In: Bolli H.M., Saunders J.B., Perch-Nielsen K. (Eds.), Plankton stratigraphy. Cambridge University Press, Cambridge, 281-314.

Jagodzinski H., 1949. Eindimensionale Fehlordnung in Kristallen Und ihr einfluss auf die röntgen interferenren. Acta Crystallographica: 2, 201-207.

Karner G.D., Watts A.B. 1983. Gravity anomalies and flexure of the lithosphere at mountain range. Journal of Geophysical Research: 88, 10449-10477.

Kneller B.C., Branney M.J. 1995. Sustained high-density turbidity currents and the deposition of thick massive sands. Sedimentology: 42, 607-616.

Krijgsman W., Hilgen F.J., Raffi I., Sierro F.J., Wilson D.S. 1999a. Chronology, causes and progression of the Messinian salinity crisis. Nature: 400, 652-655.

Krijgsman W., Hilgen F.J., Marabini S., Vai G.B. 1999b. New paleomagnetic and cyclostratigraphic age constraints on the Messinian of the Northern Apennines (Vena del Gesso Basin, Italy). Memorie della Società Geologica Italiana: 54, 25-33.

Lanson B. 1997. Decomposition of experimental X-ray diffraction patterns (profile fitting): a convenient way to study clay minerals. Clays and Clay Minerals: 45,132-146.

Lofi J., Gorini C., Berné S., Clauzon G., Dos Reis A.T., Ryan W.B.F., Steckeler M.S. 2005. Erosional processes and paleo-environmental changes in the western gulf of Lions (SW France) during the Messinian Salinity Crisis. Marine Geology: 217, 1-30.

Manzi V., Lugli S., Ricci Lucchi F., Roveri M. 2005. Deep-water clastic evaporites deposition in the Messinian Adriatic foredeep (Northern Apennines, Italy): did the Mediterranean ever dry out?. Sedimentology: 52, 875-902.

Marini M., Milli S., Moscatelli M. 2009. Facies and geometries of turbidite lobe deposits from the Messinian Laga Formation (central Apennine, Italy). In: Pascucci V., Andreucci S. (Eds.), Abstract book, 27th IAS Meeeting of Sedimentology, Alghero, September 20-23, 2009, Sassari (Italy), 264.

Mazzoli S., Deiana, G., Galdenzi, S., Cello G. 2002. Miocene fault-controlled sedimentation and thrust propagation in the previously faulted external zones of the Umbria-Marche Apennines, Italy. European Geophysical Society, Stephan Mueller Special Publication Series: 1, 301–324.

Merriman R.J., Frey M. 1999. Patterns of very low-grade metamorphism in metapelitic rocks. In: Frey M., Robinson D. (Eds.), Low grade metamorphism. Blackwell, Oxford, 61-107.

Milli S., Moscatelli M. 2000. Facies analysis and physical stratigraphy of the Messinian turbiditic complex in the Valle del Salto and Val di Varri (Central Apennines). Giornale di Geologia: 62, 57-77.

Milli S., Moscatelli M., Marini M., Stanzione O. 2009. The Messinian turbidite deposits of the Laga basin (central Apennines, Italy) In: Pascucci V., Andreucci S. (Eds.), Field Trip Guide Book, Post-conference trip FT12, 27th IAS Meeting of Sedimentology Alghero, September 20-23, 2009, Sassari (Italy), 279-297.

Milli S., Moscatelli M., Stanzione O., Falcini F. 2007. Sedimentology and physical stratigraphy of the Messinian turbidites deposits of the Laga Basin (central Apennines, Italy). Bollettino della Società Geologica Italiana: 126, 37-48.

Moore D.M., Reynolds R.C. Jr. 1997. X-Ray diffraction and the identification and analysis of clay minerals. Oxford University Press, Oxford, 378 pp.

Morelli C., 1994. Ricostruzione dell'evoluzione tettonico-sedimentaria dei bacini di avanfossa Marchigiano - Abruzzesi durante il Messiniano - Pliocene Inferiore. Ph.D Thesis, SAPIENZA Università di Roma, 300 pp.

Moscatelli M., 2003. La sedimentazione torbiditica e le sue relazioni con quella fluvio deltizia nel sistema d'avanfossa alto-miocenico dell'Appennino centro-meridionale. Ph.D Thesis, SAPIENZA Università di Roma, 320 pp.

Mostardini F., Merlini S. 1986. Appennino centro-meridionale: Sezioni geologiche e proposta di modello strutturale. Memorie della Società Geologica Italiana: 35, 177-202.

Mutti E., Sonnino M. 1981. Compensation cycles: a diagnostic features of turbidite sandstone lobes. In: Valloni R., Colella A., Sonnino M., Mutti E., Zuffa G.G., Ori G.G. (Eds.), Abstact volume Internation Association of Sedimentologists 2nd European Regional Meeting, Bologna.

Mutti E., Davoli G., Mora S., Papani L. 1994. Internal stacking pattern of ancient turbidite sytems from collisional basins. In: Weimer P., Bouma A.H., Perkins B. (Eds.), Submarine fans and turbidite systems. GCS-SEPM 15th Annual Research Conference, Austin, 257-268.

Mutti E., Nilsen T.H., Ricci Lucchi F. 1978. Outer fan depositional lobes of Laga Formation (Upper Miocene and Lower Pliocene), east central Italy. In: Stanley D.J., Kelling G. (Eds.), Sedimentation in submarine canyons, fans and trenches. Downed, Hutchinson & Ross, 210-223.

Mutti E., Tinterri R., Benevelli G., Di Biase D., Cavanna G. 2003. Deltaic, mixed and turbidite sedimentation of ancient foreland basins. Marine Petroleum Geology: 20, 733-755.

Mutti E., Tinterri R., Remacha E., Mavilla N., Angella S., Fava L. 1999. An introduction to the analysis of ancient turbidite basins from an outcrop perspective. American Association of Petroleum Geologists Continuing Educastion Course Note Series: 39, 61 pp.

Ori G.G., Serafini G., Visentin C., Ricci Lucchi F., Casnedi R., Colalongo M.L., Mosna. S. 1991. The Pliocene-Pleistocene Adriatic foredeep (Marche and Abruzzo, Italy). An integrated approach to surface and subsurface geology. 3rd E.A.P.G., Conference, Florence, Italy, Adriatic Foredeep Field Trip Guide Book, 85 pp.

Patacca E., Scandone P. 1989. Post-Tortonian mountain building in the Apennines. The role of passive sinking of a relic lithospheric slab. In: Boriani A., Bonafede M., Piccardo G.B., Vai G.B. (Eds.), The lithosphere in Italy. Roma, CNR-Accademia Nazionale dei Lincei, 115-170.

Patacca E., Sartori R., Scandone P. 1993. Tyrrhenian basin and Apennines kinematics evolution and related dynamics constraints. In: Boschi E., Mantovani E., Morelli,A. (Eds.), Recent evolution on the Mediterranean region. Kluwier Academic Publication, 161-171.

Pollastro R.M. 1993. Consideration and applications of the illite/smectite geothermometer in hydrocarbon-bearing rocks of Miocene to Mississipian age. Clays and Clay Minerals: 41, 119-133.

Price L.C. 1983. Geologic time as a parameter in organic metamorphism and vitrinite reflectance as an absolute paleogeothermometer. Journal of Petroleum Geology: 6, 5-38.

Ricci Lucchi F. 1986. The Oligocene to Recent foreland basins of the Northern Apennines. In: Allen P.A., Homewood P. (Eds.), Foreland basins. International Association of Sedimentologists, Special Publication: 8, 105-139.

Ricci Lucchi F., Colalongo M.L., Cremonini G., Gasperi G., Iaccarino S., Papani G., Raffi S., Rio D. 1982. Evoluzione sedimentaria e paleogeografica del margine appenninico. In: Cremonini G., Ricci Lucchi F. (Eds.), Guida alla geologia del margine appenninico-padano. Società Geologica italiana, Bologna, 17-46.

Ronchi P., Casaglia F., Ceriani A. 2003. The multiphase dolomitization of the Liassic Calcare Massiccio e Corniola successions (Montagna dei Fiori, Northern Apennines, Italy). Bollettino della Società Geologica Italiana: 122, 157-172.

Royden L., Karner G.D. 1984. Flexure of the lithosphere beneath Apennine and Carpathian foredeep basins: evidence for an insufficient topographic load. American Association of Petroleum Geologists Bulletin: 68, 704-712.

Roveri M., Manzi V. 2006. The Messinian salinity crisis: looking for a new paradigm?. Palaeogeography, Palaeoclimatology, Palaeoecology: 238, 386-398.

Roveri M., Bassetti M.A., Ricci Lucchi F. 2001. The Mediterranean Messinian salinity crisis: an Apennine foredeep perspective. Sedimentary Geology: 140, 201-214.

Roveri M., Lugli S., Manzi V., Schreiber C. 2008. The Messinian salinity crisis: a sequence-stratigraphic approach. In: Amorosi A., Haq B.U., Sabato L. (Eds.), Advances in application of sequence stratigraphy in Italy. GeoActa, Special Publication: 1, 117-138.

Roveri M., Manzi V., Ricci Lucchi F., Rogledi S. 2003. Sedimentary and tectonic evolution of the Vena del Gesso Basin (Northern Apennines, Italy): implications for the onset of the Messinian Salinity Crisis. Geological Society of America Bulletin: 115, 387-405.

Roveri M., Ricci Lucchi F., Lucente C.C., Manzi V., Mutti E. 2002. Stratigraphy, facies and basin fill history of the Marnoso-arenacea Formation. In: Mutti E., Ricci Lucchi F., Roveri M. (Eds.), Revisiting turbidites of the Marnoso-arenacea Formation and their basin-margin equivalents: problems with classic models. 64th EAGE Conference and Exhibition. Excursion Guidebook, University of Parma and ENI, AGIP Division, 1-26.

Rusciadelli G., Viandante M.G., Calamita F., Cook A.C. 2005. Burial-exhumation history of the central Apennines (Italy), from the foreland to the chain building: thermochronological and geological data. Terra Nova: 17, 34-38.

Ryan W.B.F., Cita M.B. 1978. The nature and distribution of Messinian Erosional Surface; indicators of a several-kilometer-deep Mediterranean in the Miocene. Marine Geology: 27, 193-230.

Scisciani V., Montefalcone R. 2005. Evoluzione neogenico-quaternaria del fronte della catena centro-appenninica: vincoli dal bilanciamento sequenziale di una sezione geologica regionale. Bollettino della Società Geologica Italiana: 124, 579-599.

Sparks R.S.J., Bonnecaze R.T., Huppert H.E., Lister J.R., Hallworth M.A., Mader H., Phillips J. 1993. Sediment-laden gravity currents with reversing buoyancy. Earth and Planetary Science Letters: 114, 243-257.

Speranza F., Adamoli L., Maniscalco R., Florindo F. 2003. Genesis and evolution of a curved mountain front: paleomagnetic and geological evidence from Gran Sasso range (Central Apennines, Italy). Tectonophysics: 362, 183-197.

Srodo J. 1999. Nature of mixed-layer clays and mechanisms of their formation and alteration. Annual Review of Earth and Planetary Sciences: 27, 19-53.

Stanzione O. 2007. Analisi di facies e stratigrafia fisica dei depositi torbiditici del Messiniano inferiore della formazione della Laga. Ph.D Thesis, SAPIENZA Università di Roma, 175 pp.

Tavarnelli E., Butler R.W.H., Decandia F.A., Calamita F., Grasso M., Alvarez W., Renda P. 2004. Implication of fault reactivation and structural inheritance in the Cenozoic tectonic evolution of Italy. In: Crescenti U., D'Offizi S., Merlino S., Sacchi L. (Eds.), Geology of Italy. Special Publication of the Italian Geological Society for the IGC 32nd. Florence, 2004, 209-222.

Tinterri R., Muzzi Magalhaes P. 2009. The Miocene turbidite deposits of the Marnoso-arenacea Fromation (northern Apennines, Italy). In: Pascucci V., Andreucci S. (Eds.), Field Trip Guide Book, Post-conference trip FT12, 27th IAS Meeting of Sedimentology Alghero, September 20-23, 2009, Sassari (Italy), 249-277.

Tozer R.S.J., Butler R.W.H., Corrado S. 2002. Comparing thin- and thick-skinned thrust tectonic models of the Central Apennines, Italy. European Geophysical Society Stefan Müller Special Publication: 1, 281-301.

Vai G.B. 1988. A field trip guide to the Romagna Apennines geology.The Lamone valley. In: De Giuli C, Vai G.B. (Eds.), Fossil vertebrates in the Lamone valley, Romagna Apennines. International workshop: continental fauna at the Mio-Pliocene boundary. Faenza, March 28-31, 1988, guidebook, 7-37.

Valloni R., Cipriani N., Morelli C. 2002. Petrostratigraphic record of the Apennine foredeep basins. Italy. Bollettino della Società Geologica Italiana: 1, 455-465.

Van Couvering J.A., Castrodori D., Cita M.B., Hilgen F.J., Rio D. 2000. The base of the Zanclean stage and of the Pliocene series. Episodes: 23, 179-187.

Warr L.N., Rice A.H.N. 1994. Inter laboratory standardization and calibration of clay mineral crystallinity and crystallite size data. Journal of Metamorphic Geology: 12, 141-152.

Appendix - methods

Clay mineralogy

XRD analyses were performed with a Scintag X_1 XRD system (CuKα radiation, solid state detector, spinning sample) at 40 kV and 45 mA. Randomly-oriented whole-rock powders were run in the 2-70°2θ interval with a step size of 0.05 °2θ and a counting time of 3 s per step. Oriented air-dried samples were scanned from 1 to 48 °2θ with a step size of 0.05 °2θ and a count time of 4 s per step. The presence of expandable clays was determined for samples treated with ethylene glycol at 25°C for 24h. Ethylene-glycol solvated samples were scanned at the same conditions as air-dried aggregates with a scanning interval of 1-30 °2θ.

Expandability measurements in the <2 µm grain-size fraction were determined according to Moore and Reynolds (1997) using the delta two-theta method after decomposing the composite peaks between 9-10°2θ and 16-17°2θ using Pearson VII functions. The I-S ordering type (Reichweite parameter, R; Jagodzinski, 1949) was determined by the position of the I 001-S 001 reflection between 5 and 8.5°2θ (Moore and Reynolds, 1997).

'Illite crystallinity' measurements expressed as Kübler index (KI) are made by interpolating the background under the peak by connecting the background on both sides of the peak and by using a profile fitting method (Lanson, 1997). Half-peak widths were calibrated using Warr and Rice's standards (1994).

Vitrinite reflectance

Mean random vitrinite reflectance was measured on whole rock samples rich in coaly particles collected from sandstone, siltstone and clayey lithologies. Samples were first mounted in epoxy resin and then polished. Vitrinite reflectance analyses were then performed on randomly oriented grains using a Zeiss Axioplan microscope and conventional microphotometric methods (e.g., under oil immersion in reflected monochromatic non-polarised light). In most cases the samples population was a few tens of readings per sample on fragments never smaller than 5 nm and only slightly fractured and/or altered. Mean reflectance and standard deviation values were calculated for all measurements.

Rock eval

Tmax, S1, S2 and S3 peaks were derived from standardized procedures of Rock Eval pyrolisis. Samples derive from surface and subsurface (Varoni 1 well) sections located in Figure 3, analyzed by Elf and discussed in Albouy et al. (2003). Presented data are selected according to Espitalié (1986).